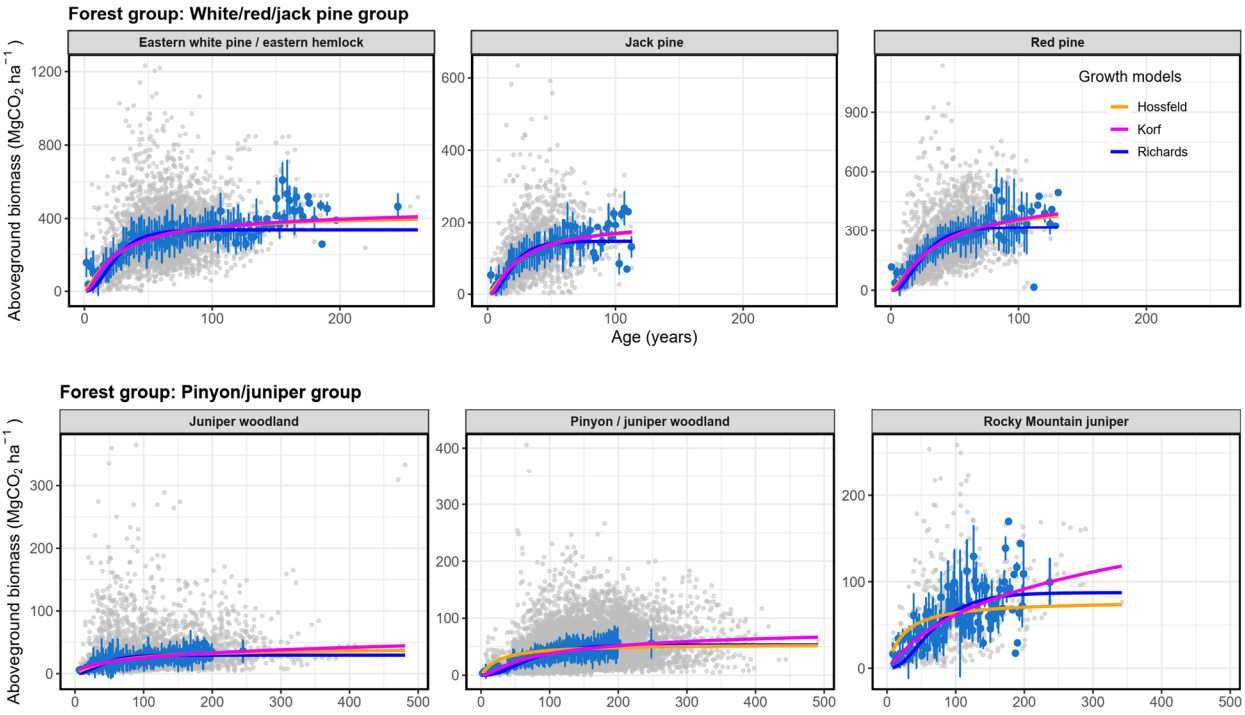

Fig S1: Changes in aboveground biomass (AGB) as a function of stand age for the white/red/jack pine forest group and the pinyon/juniper Forest group. Each panel represents a specific forest type. Gray dots depict observed data at the plot level, while blue error bars show the mean and standard deviation of AGB estimates within specific age bins. The fitted growth curves are distinguished by colors: Hossfeld (orange), Korf (magenta), and Chapman-Richards (blue).

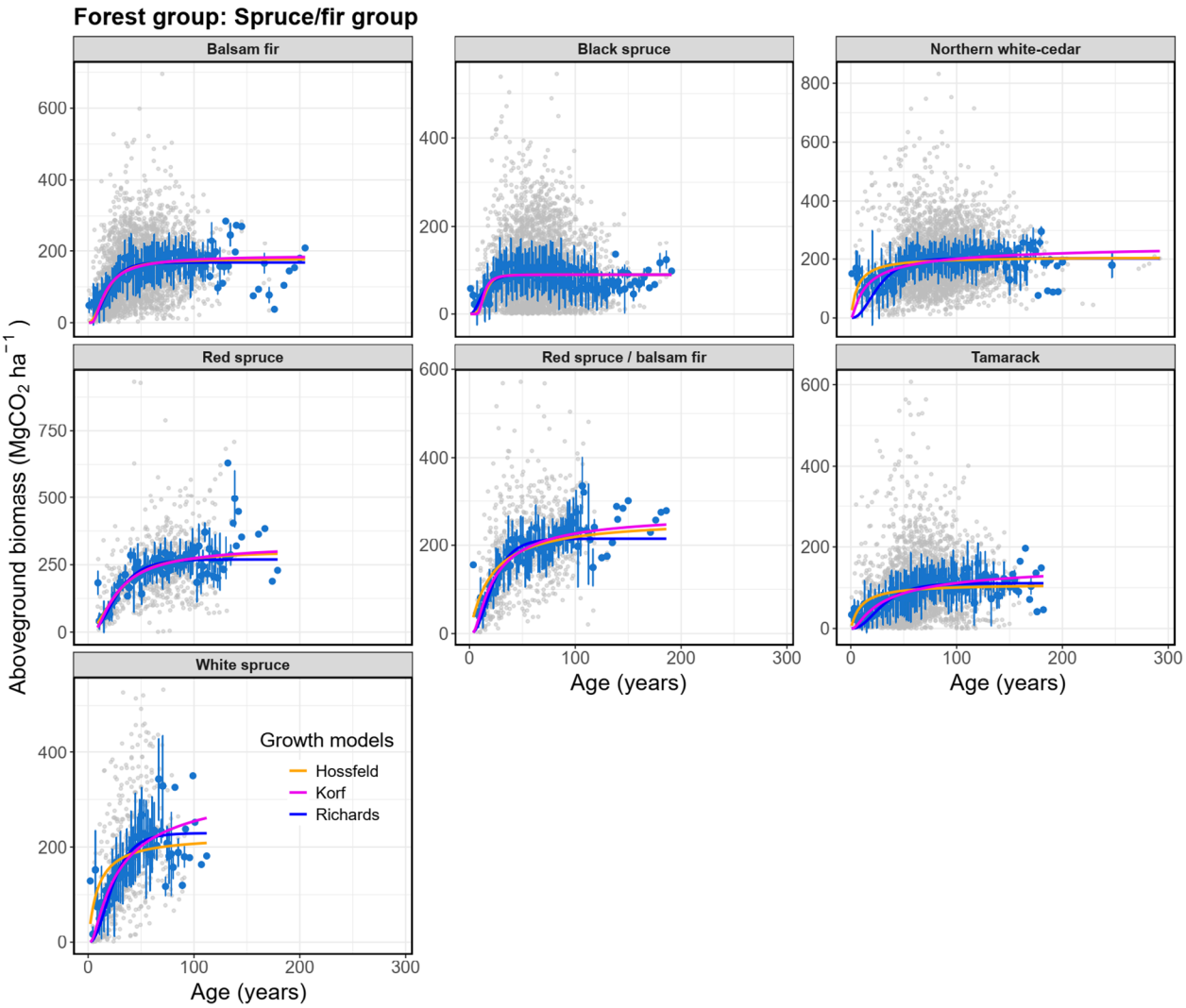

Fig S2: Changes in aboveground biomass (AGB) as a function of stand age for the spruce/fir forest group. Each panel represents a specific forest type. Gray dots depict observed data at the plot level, while blue error bars show the mean and standard deviation of AGB estimates within specific age bins. The fitted growth curves are distinguished by colors: Hossfeld (orange), Korf (magenta), and Chapman-Richards (blue).

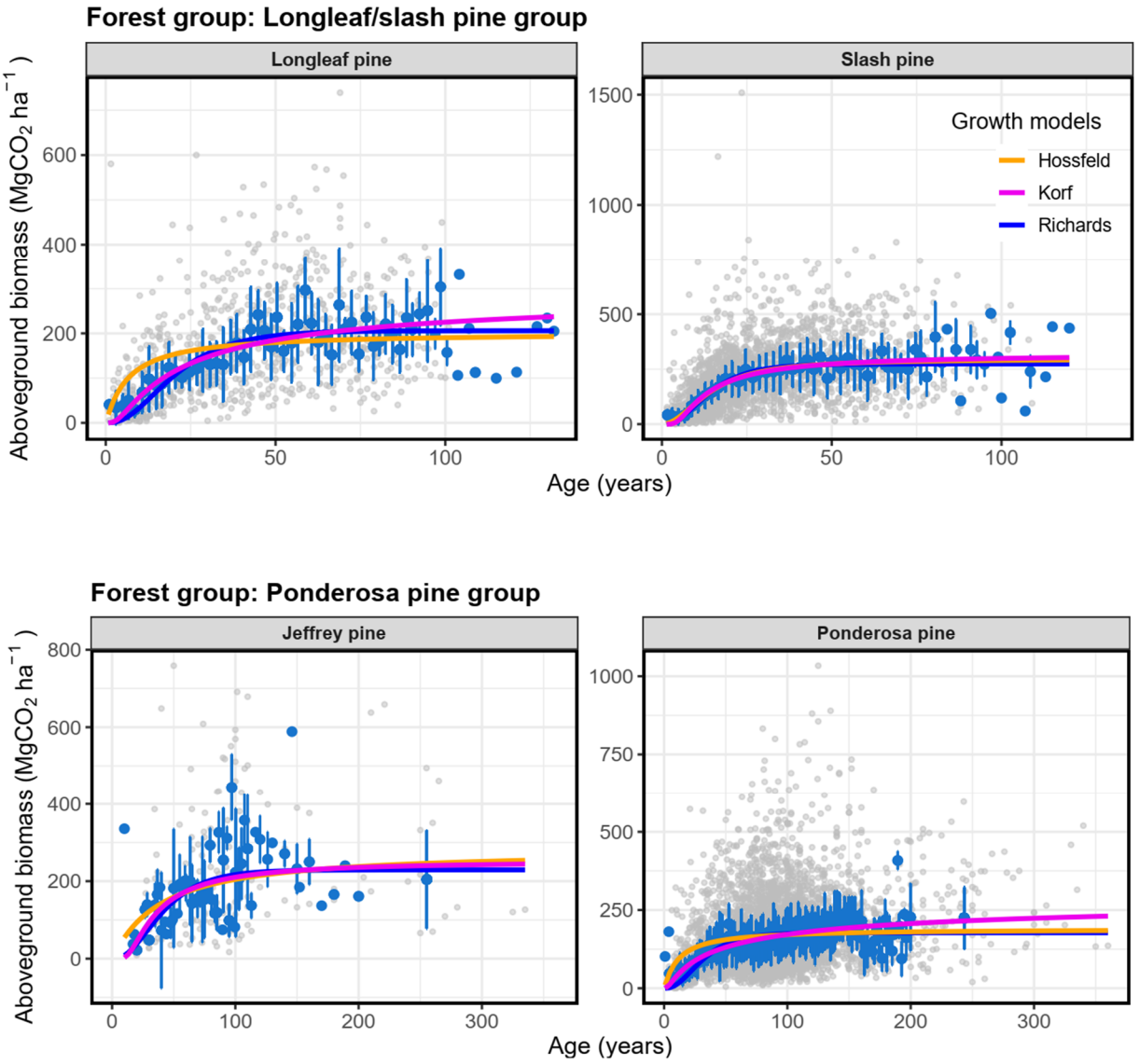

Fig S3: Changes in aboveground biomass (AGB) as a function of stand age for the longleaf/slash pine forest group and the ponderosa pine forest group. Each panel represents a specific forest type. Gray dots depict observed data at the plot level, while blue error bars show the mean and standard deviation of AGB estimates within specific age bins. The fitted growth curves are distinguished by colors: Hossfeld (orange), Korf (magenta), and Chapman-Richards (blue).

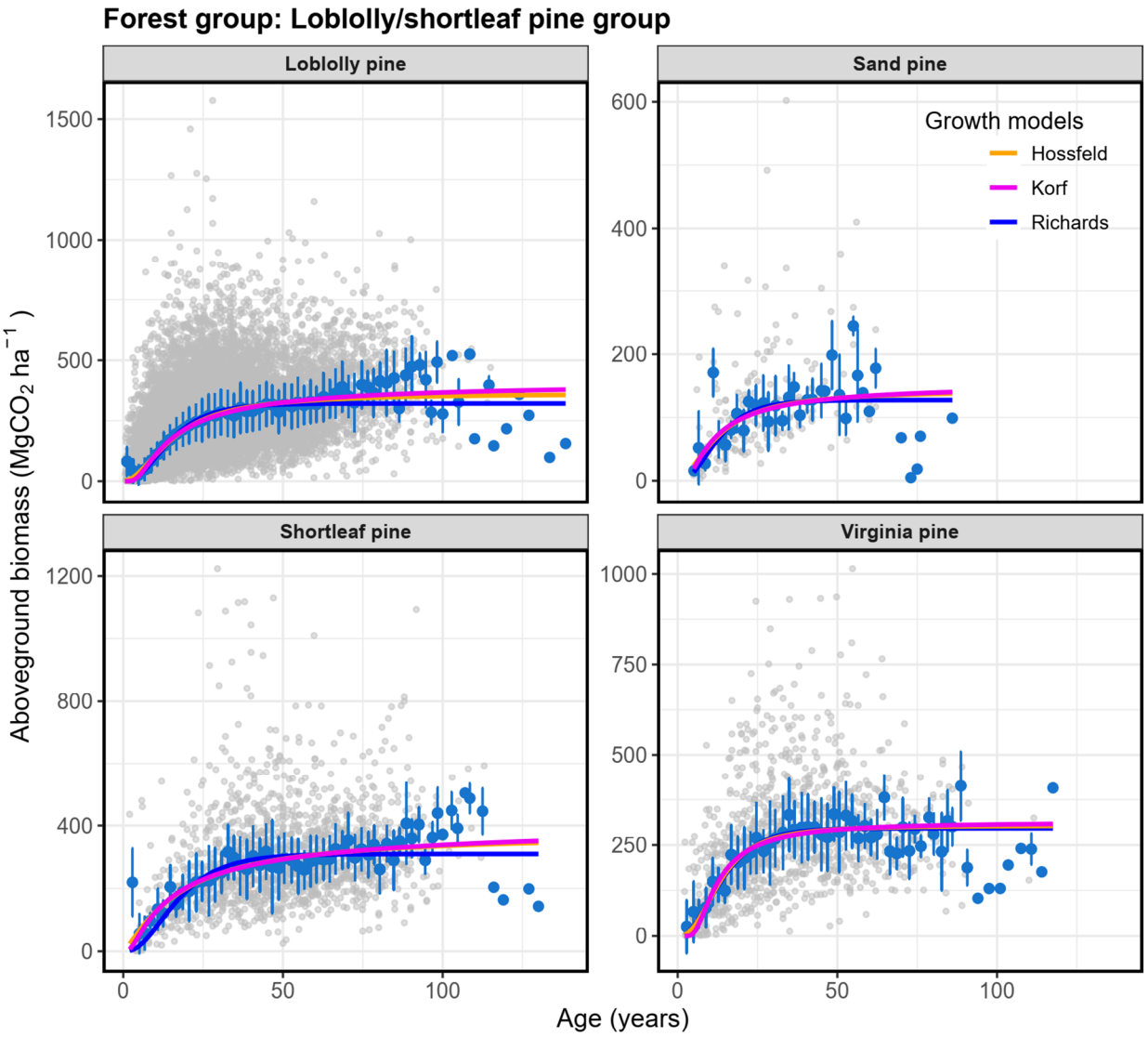

Fig S4: Changes in aboveground biomass (AGB) as a function of stand age for the loblolly/shortleaf pine forest group. Each panel represents a specific forest type. Gray dots depict observed data at the plot level, while blue error bars show the mean and standard deviation of AGB estimates within specific age bins. The fitted growth curves are distinguished by colors: Hossfeld (orange), Korf (magenta), and Chapman-Richards (blue).

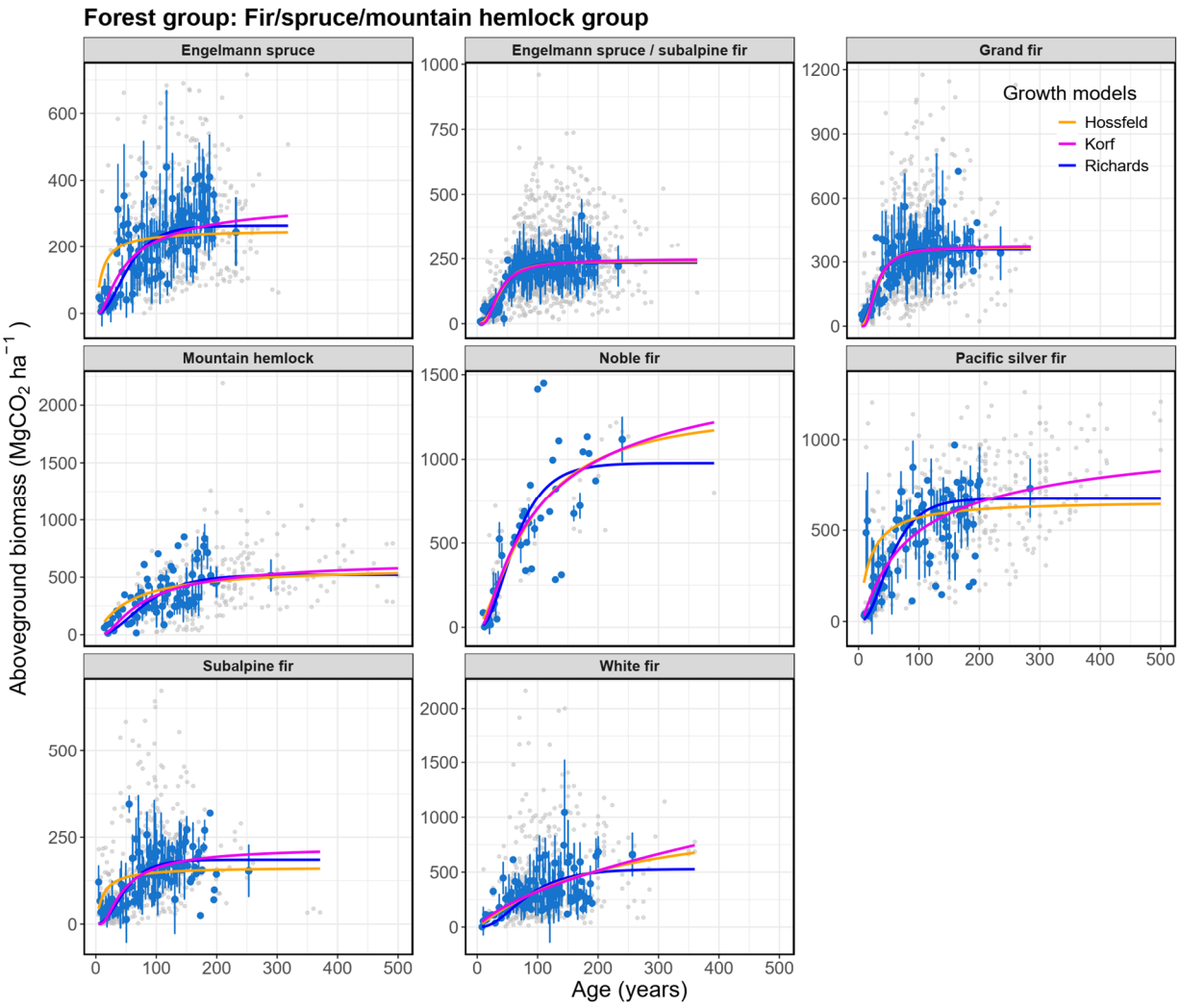

Fig S5: Changes in aboveground biomass (AGB) as a function of stand age for the fir/spruce/mountain hemlock forest group. Each panel represents a specific forest type. Gray dots depict observed data at the plot level, while blue error bars show the mean and standard deviation of AGB estimates within specific age bins. The fitted growth curves are distinguished by colors: Hossfeld (orange), Korf (magenta), and Chapman-Richards (blue).

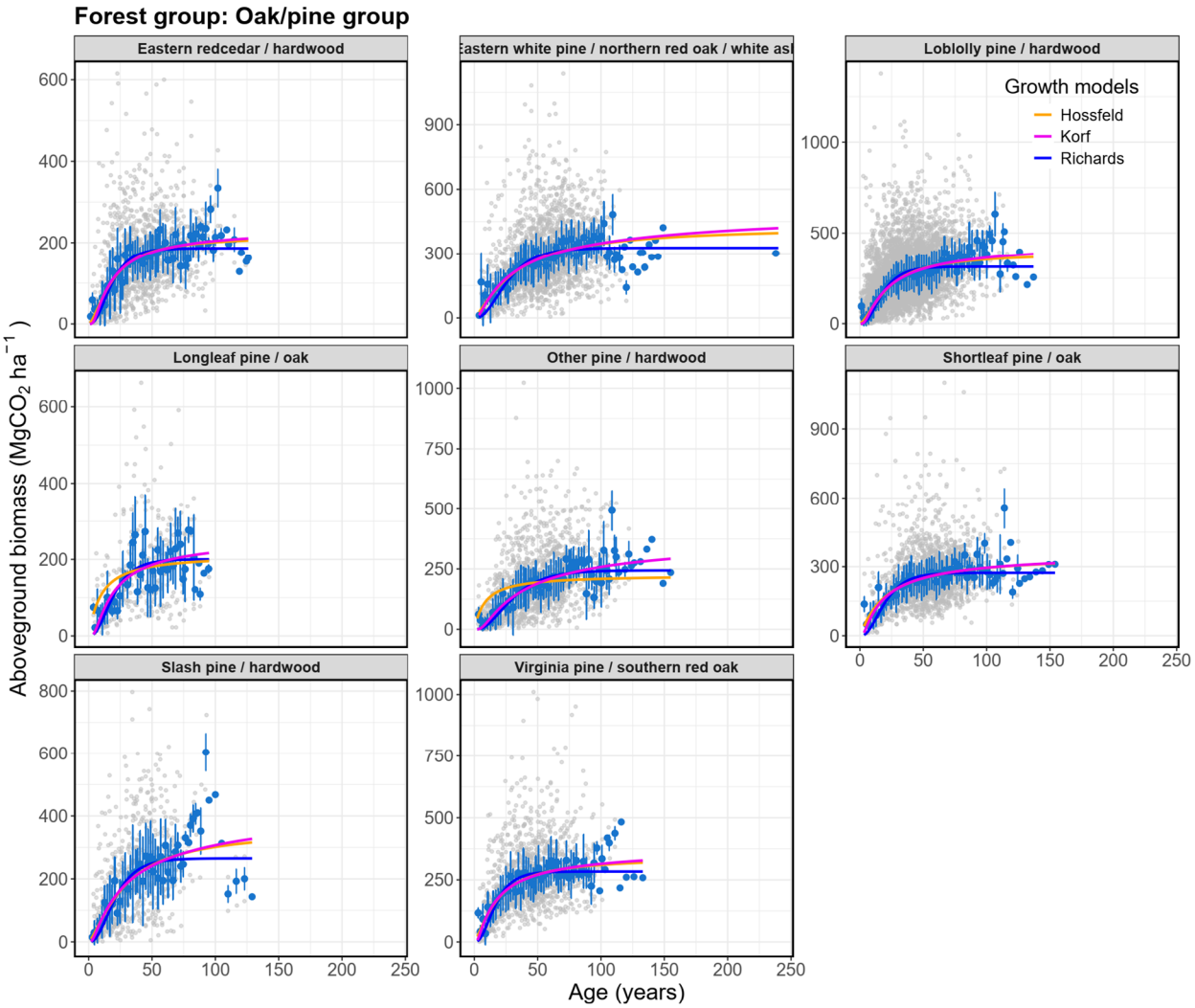

Fig S6: Changes in aboveground biomass (AGB) as a function of stand age for the oak/pine forest group. Each panel represents a specific forest type. Gray dots depict observed data at the plot level, while blue error bars show the mean and standard deviation of AGB estimates within specific age bins. The fitted growth curves are distinguished by colors: Hossfeld (orange), Korf (magenta), and Chapman-Richards (blue).

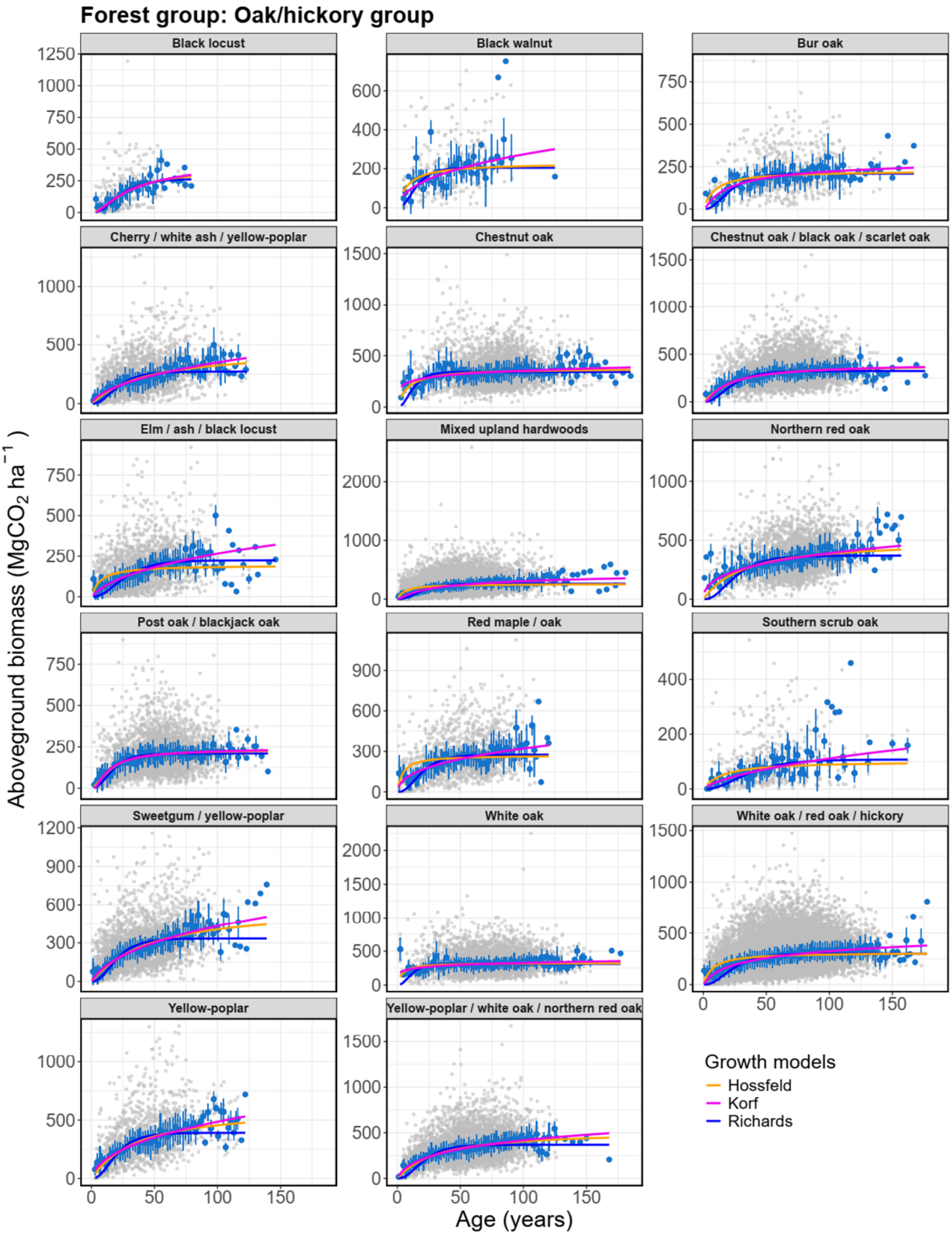

Fig S7: Changes in aboveground biomass (AGB) as a function of stand age for the oak/hickory forest group. Each panel represents a specific forest type. Gray dots depict observed data at the plot level, while blue error bars show the mean and standard deviation of AGB estimates within specific age bins. The fitted growth curves are distinguished by colors: Hossfeld (orange), Korf (magenta), and Chapman-Richards (blue).

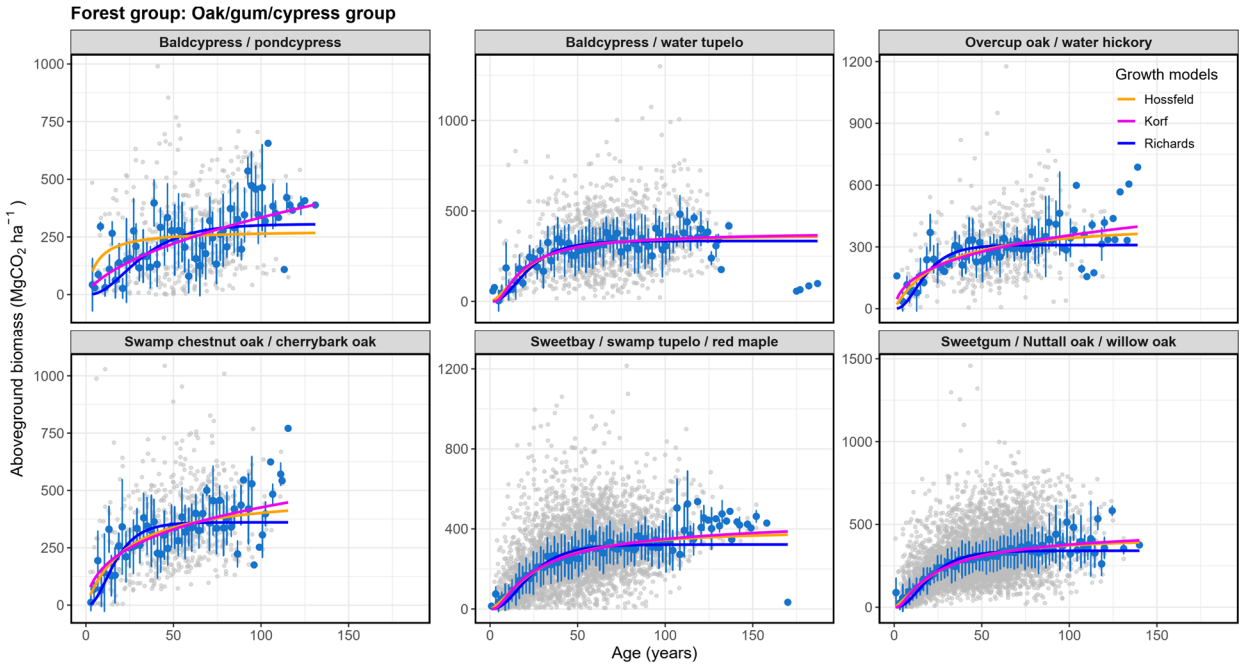

Fig S8: Changes in aboveground biomass (AGB) as a function of stand age for the oak/gum/cypress forest group. Each panel represents a specific forest type. Gray dots depict observed data at the plot level, while blue error bars show the mean and standard deviation of AGB estimates within specific age bins. The fitted growth curves are distinguished by colors: Hossfeld (orange), Korf (magenta), and Chapman-Richards (blue).

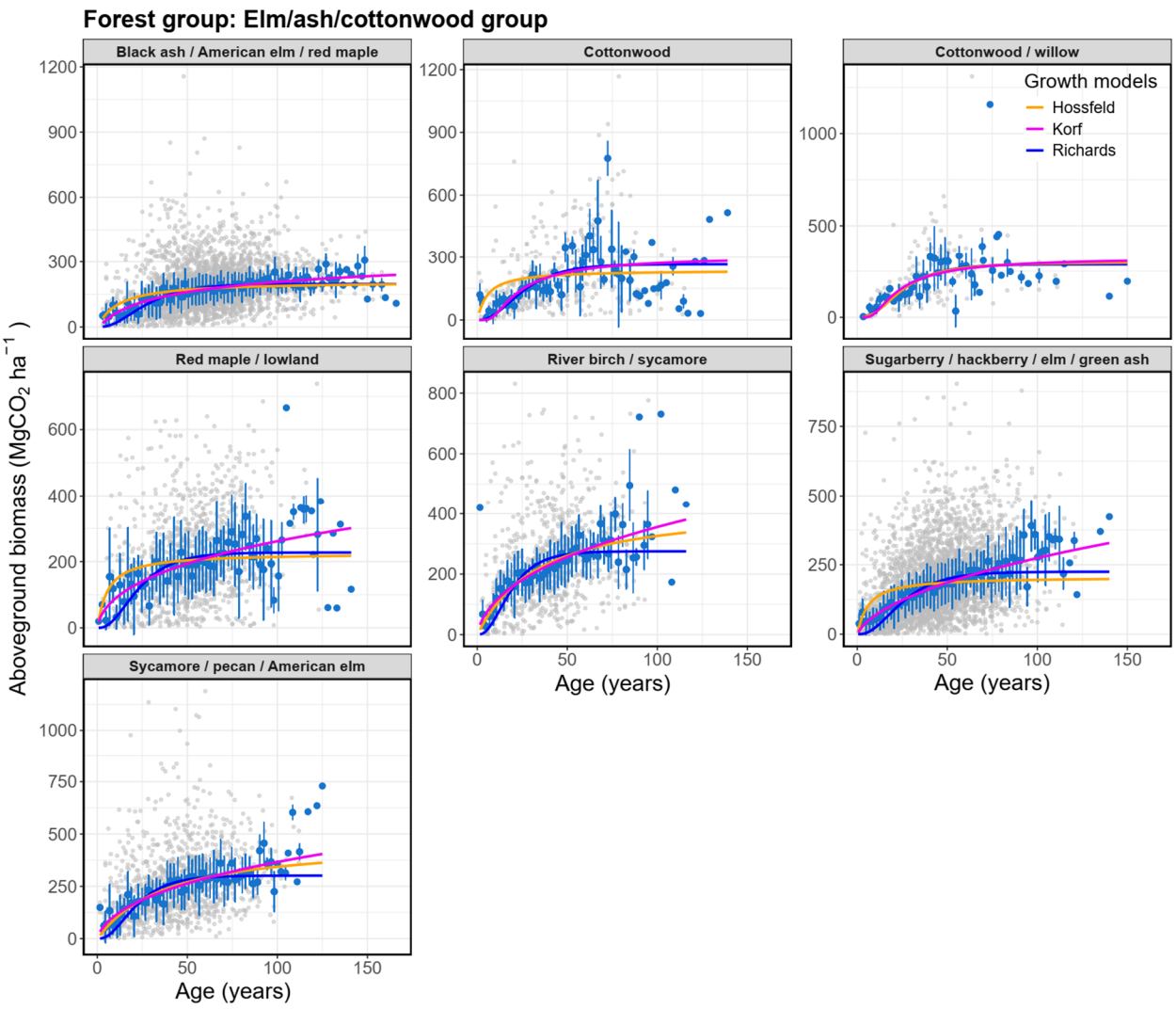

Fig S9: Changes in aboveground biomass (AGB) as a function of stand age for the elm/ash/cottonwood forest group. Each panel represents a specific forest type. Gray dots depict observed data at the plot level, while blue error bars show the mean and standard deviation of AGB estimates within specific age bins. The fitted growth curves are distinguished by colors: Hossfeld (orange), Korf (magenta), and Chapman-Richards (blue).

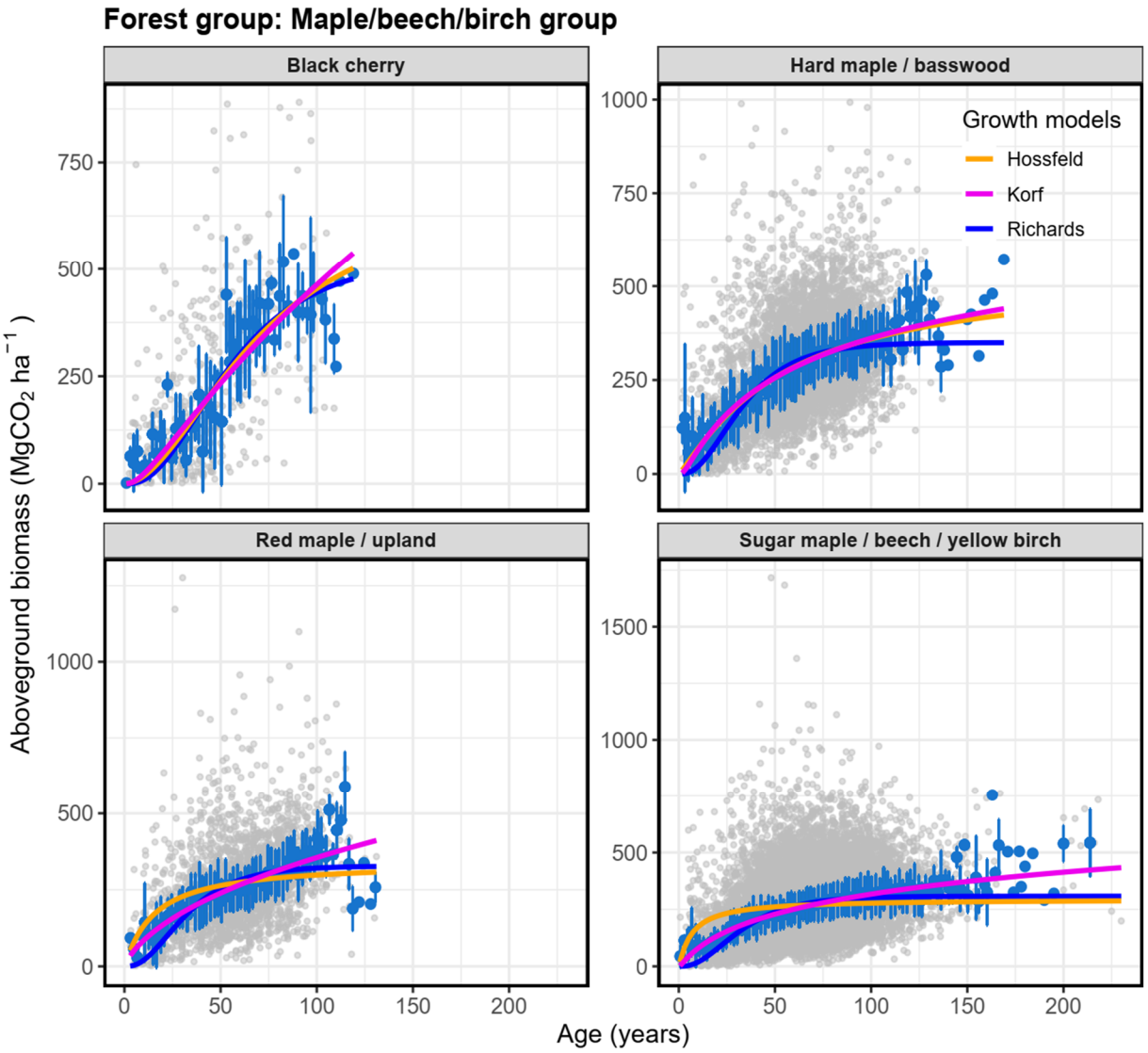

Fig S10: Changes in aboveground biomass (AGB) as a function of stand age for the maple/beech/birch forest group. Each panel represents a specific forest type. Gray dots depict observed data at the plot level, while blue error bars show the mean and standard deviation of AGB estimates within specific age bins. The fitted growth curves are distinguished by colors: Hossfeld (orange), Korf (magenta), and Chapman-Richards (blue).

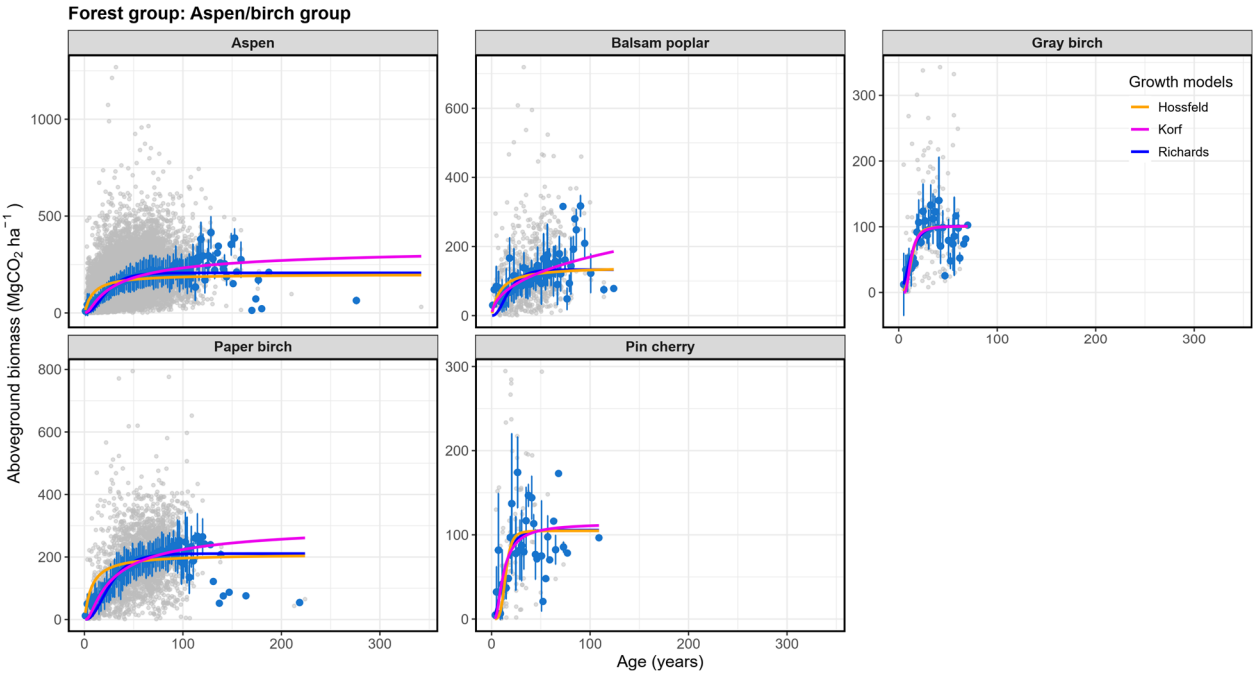

Fig S11: Changes in aboveground biomass (AGB) as a function of stand age for the aspen/birch forest group. Each panel represents a specific forest type. Gray dots depict observed data at the plot level, while blue error bars show the mean and standard deviation of AGB estimates within specific age bins. The fitted growth curves are distinguished by colors: Hossfeld (orange), Korf (magenta), and Chapman-Richards (blue).

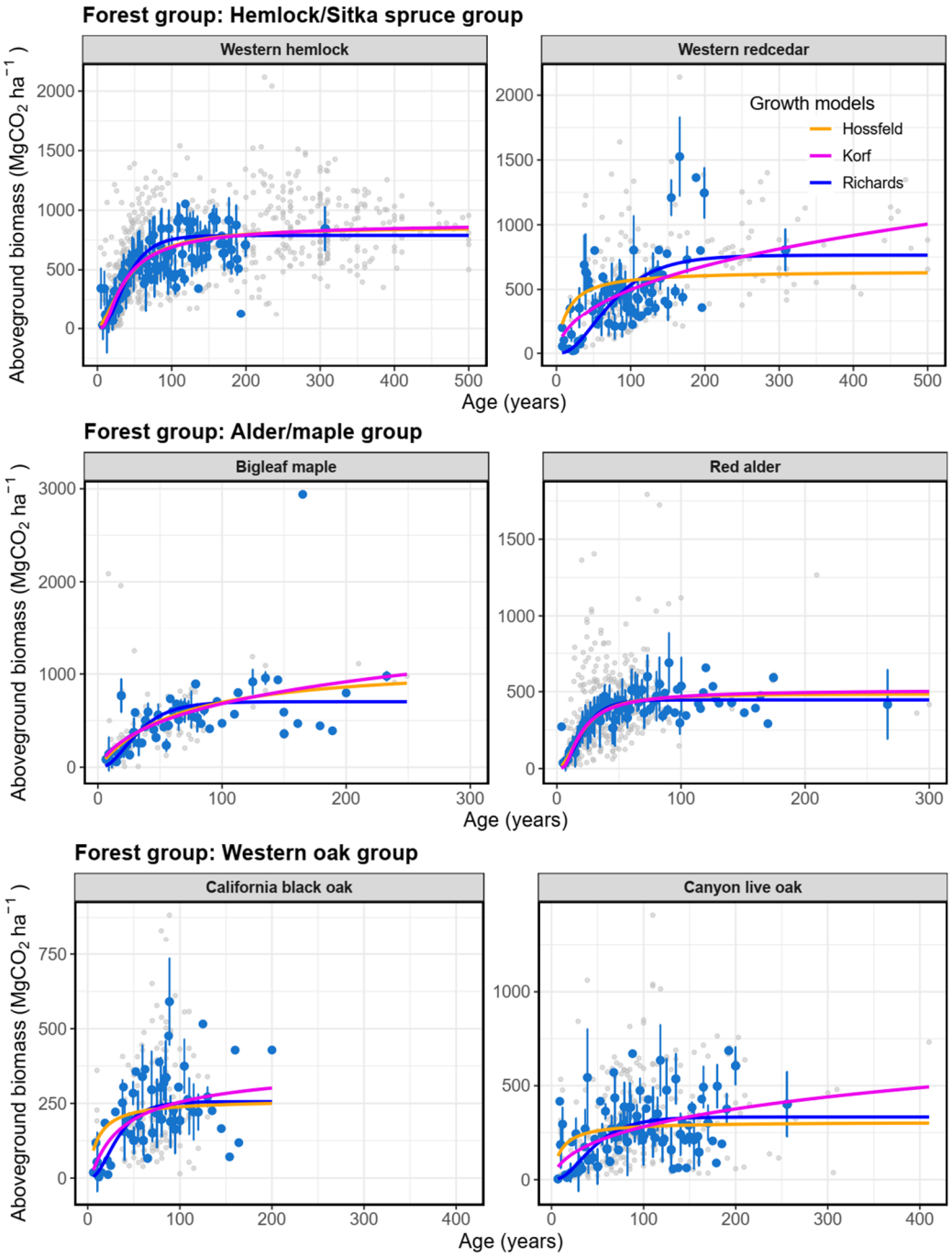

Fig S12: Changes in aboveground biomass (AGB) as a function of stand age for the hemlock/sitka spruce forest group, alder/maple forest group, and western oak forest group. Each panel represents a specific forest type. Gray dots depict observed data at the plot level, while blue error bars show the mean and standard deviation of AGB estimates within specific age bins. The fitted growth curves are distinguished by colors: Hossfeld (orange), Korf (magenta), and Chapman-Richards (blue).

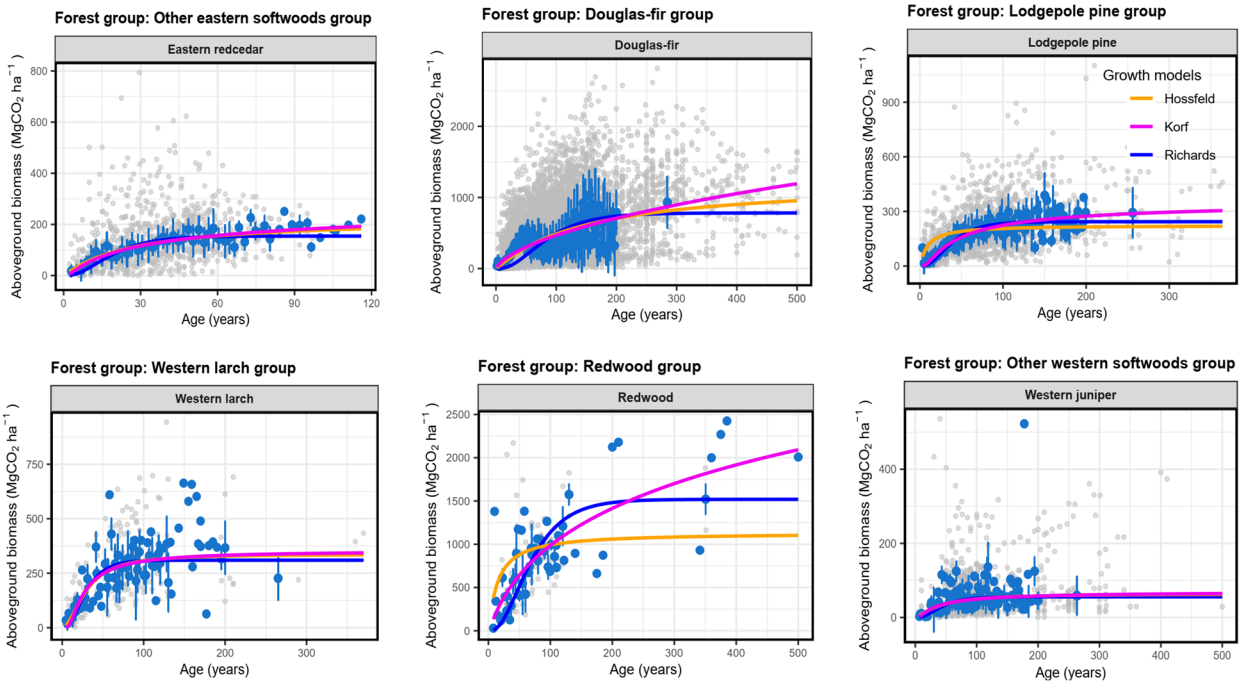

Fig S13: Changes in aboveground biomass (AGB) as a function of stand age for six different forest groups. Each panel represents a specific forest type. Gray dots depict observed data at the plot level, while blue error bars show the mean and standard deviation of AGB estimates within specific age bins. The fitted growth curves are distinguished by colors: Hossfeld (orange), Korf (magenta), and Chapman-Richards (blue).

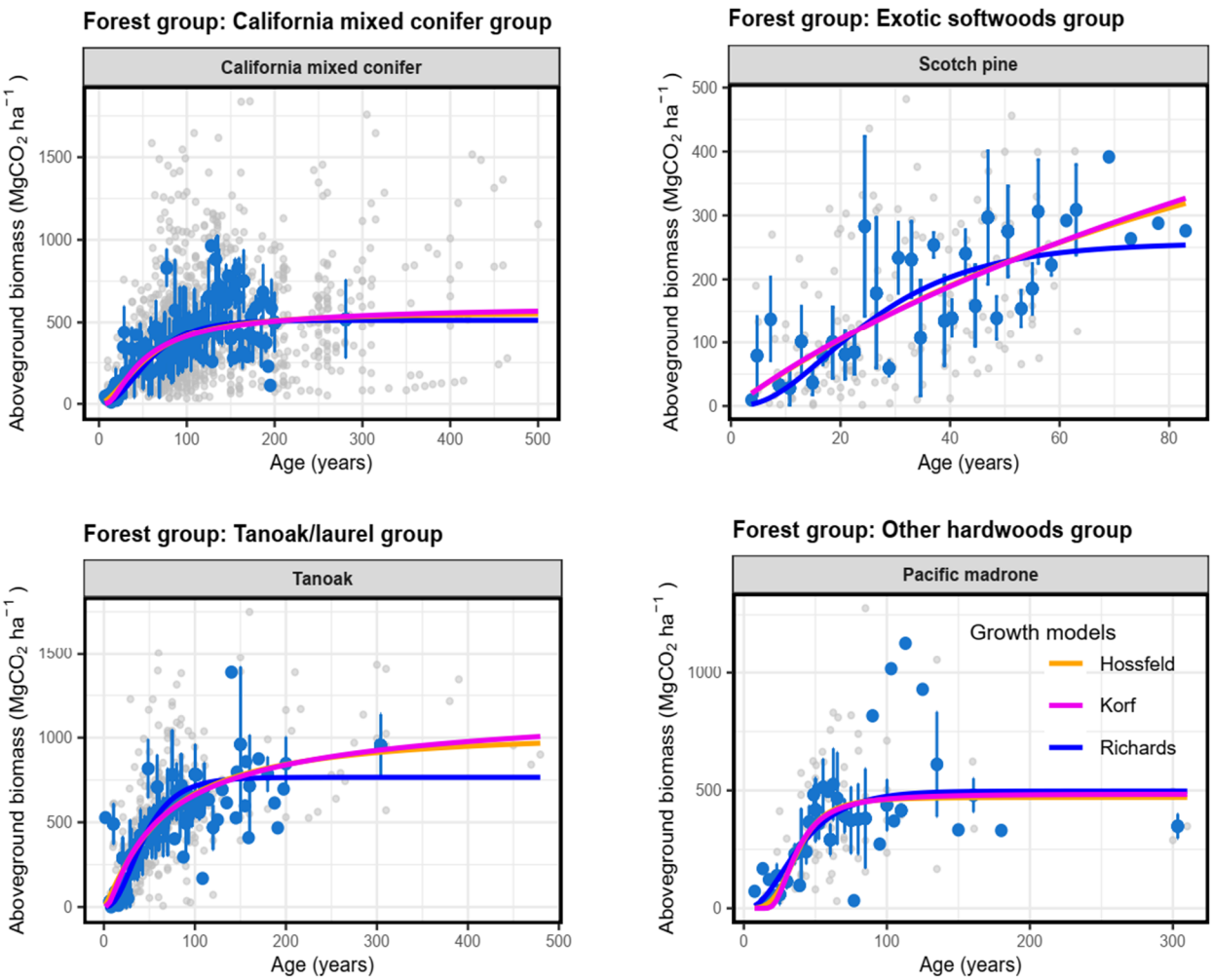

Fig S14: Changes in aboveground biomass (AGB) as a function of stand age for four different forest groups. Each panel represents a specific forest type. Gray dots depict observed data at the plot level, while blue error bars show the mean and standard deviation of AGB estimates within specific age bins. The fitted growth curves are distinguished by colors: Hossfeld (orange), Korf (magenta), and Chapman-Richards (blue).

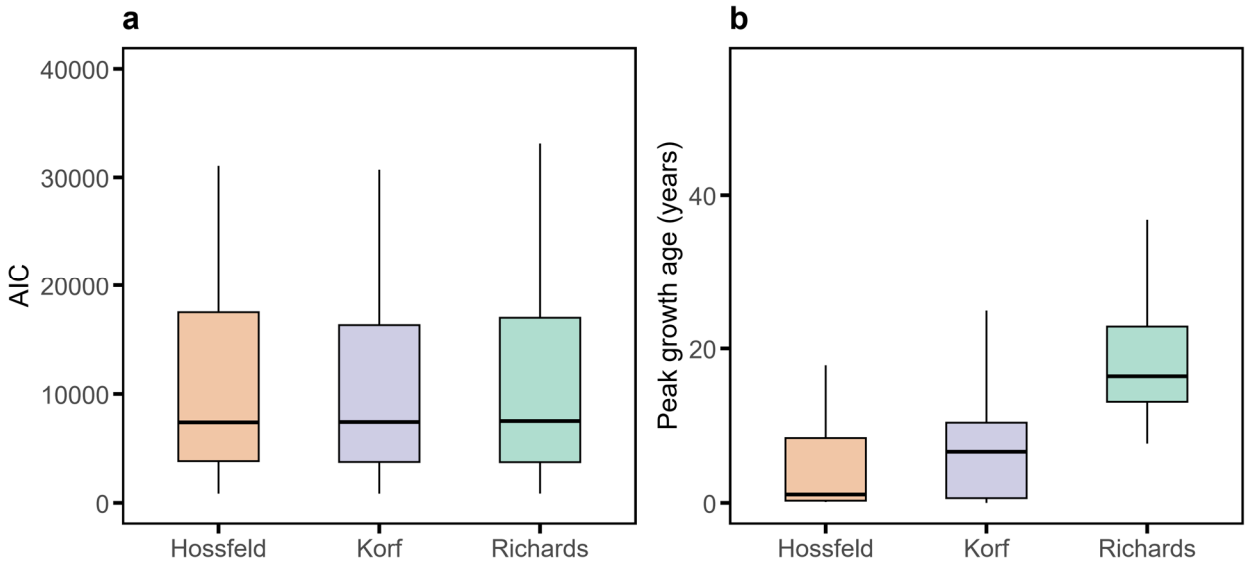

Fig S15: Model comparison across 92 forest types. a. Distributions of Akaike information criterion (AIC) values for fits using the Hossfeld, Korf, and Chapman–Richards growth functions. **b.** Corresponding distributions of peak growth age derived from the fitted parameters for each model. Boxplots show medians and interquartile ranges; whiskers indicate the full range across forest types.

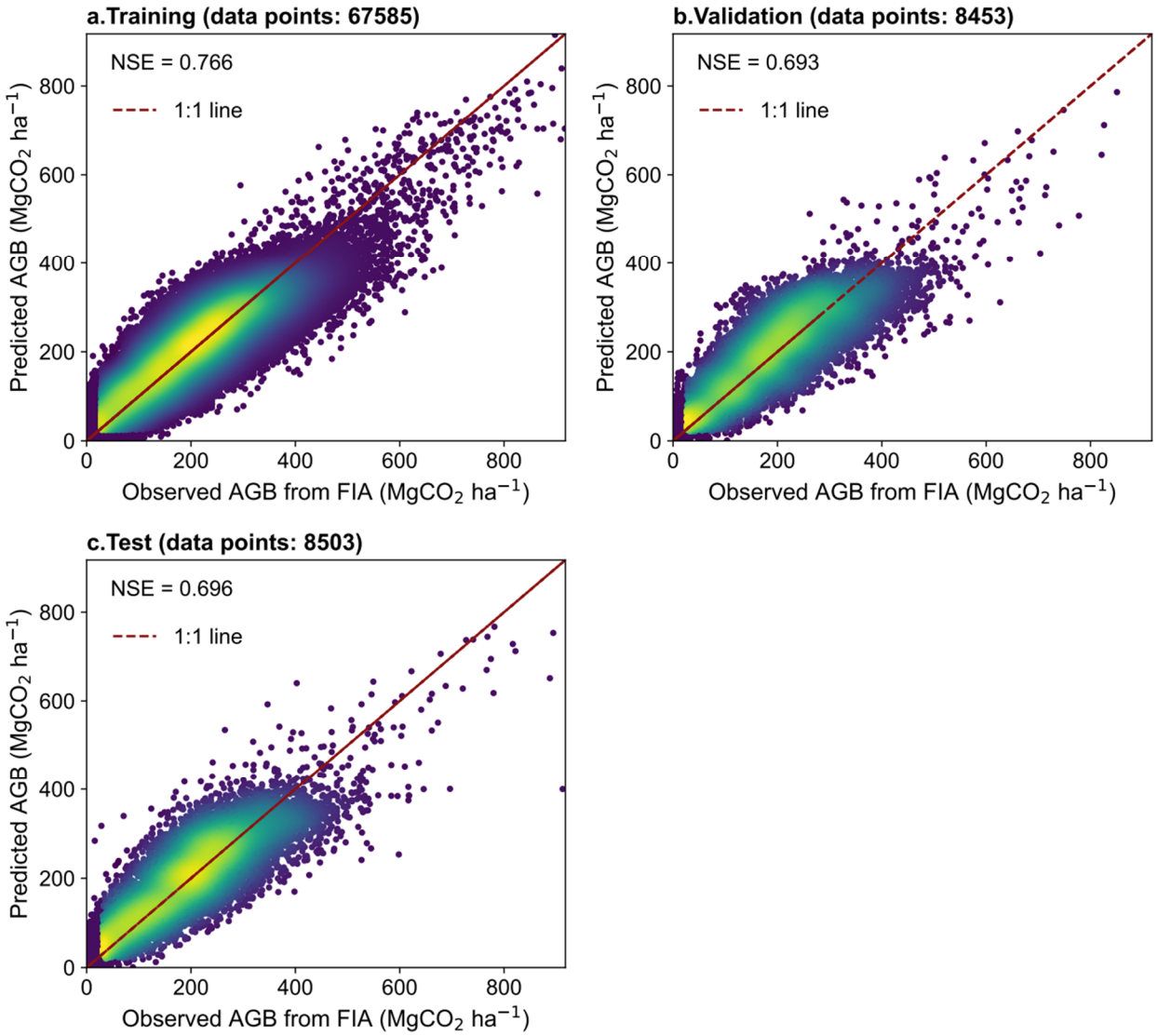

Fig S16: Comparison of observed aboveground biomass (AGB) with simulated AGB generated by the Biogeochemistry-Informed Neural Network (BINN) for the training, validation and test. The scatter plot visualizes the relationship between observed and simulated values, with a color gradient indicating the density of data points. The red line represents the linear regression fit, while the green line corresponds to the identity function (1:1 line).

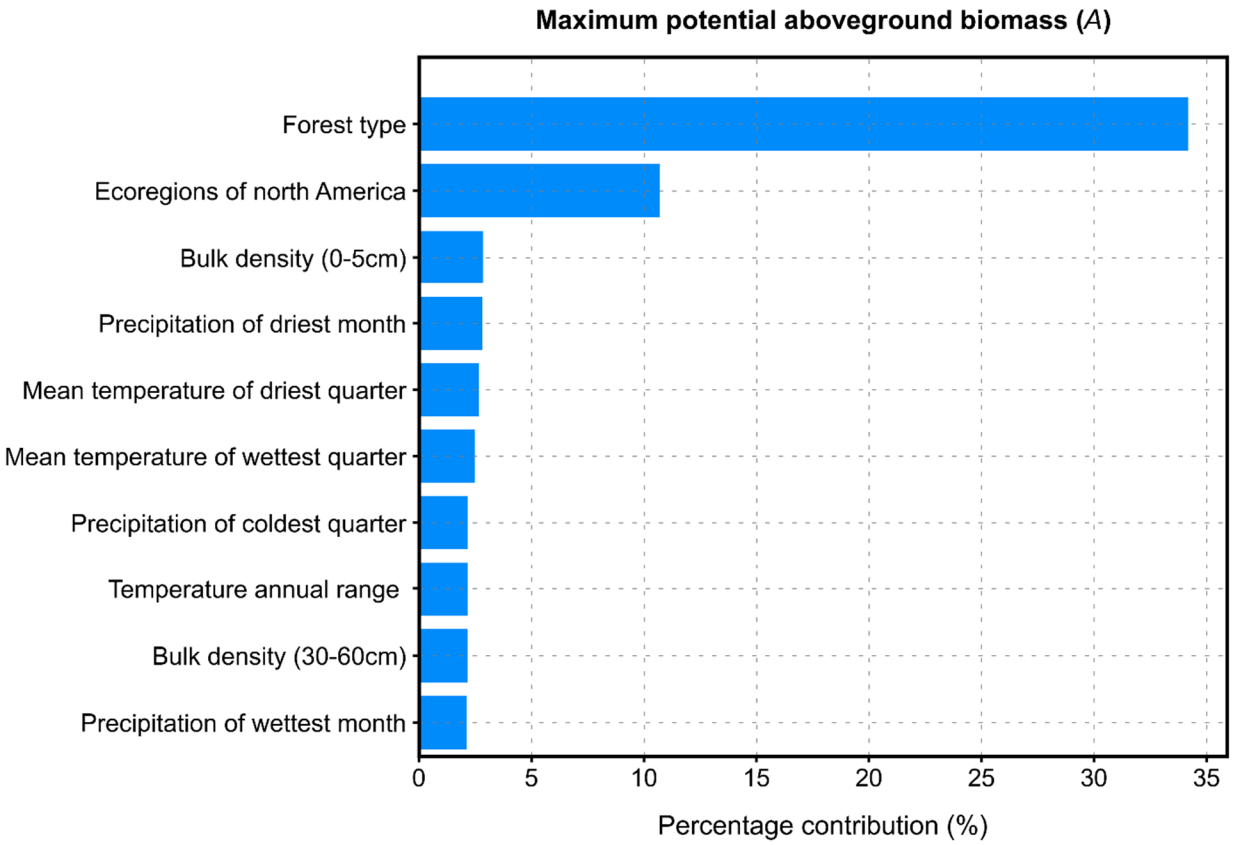

Fig S17: The percentage contributions of the top 10 covariates to the spatial variation of the *A* parameter in the Chapman-Richards growth function. The *A* parameter represents the maximum potential aboveground biomass.

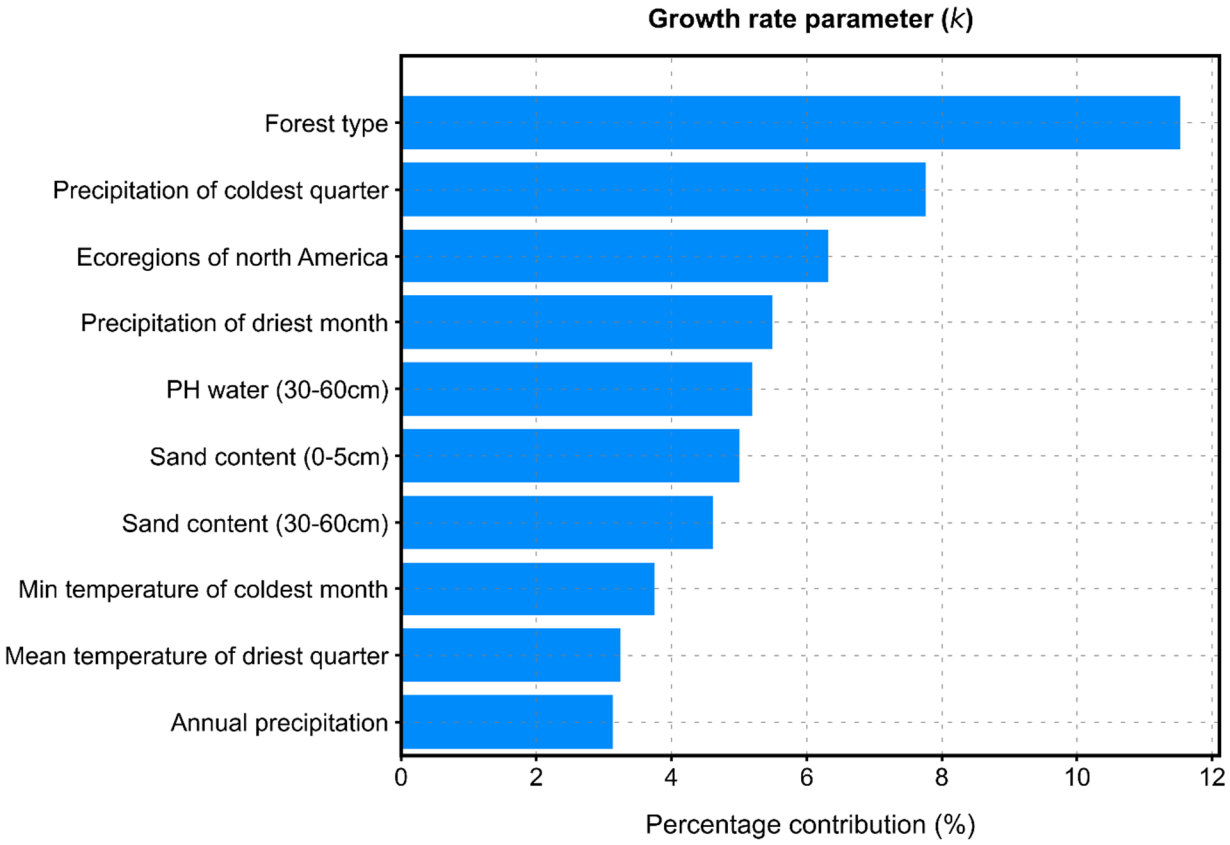

Fig S18: The percentage contributions of the top 10 covariates to the spatial variation of the *k* parameter in the Chapman-Richards growth function. The *k* parameter represents the growth rate.

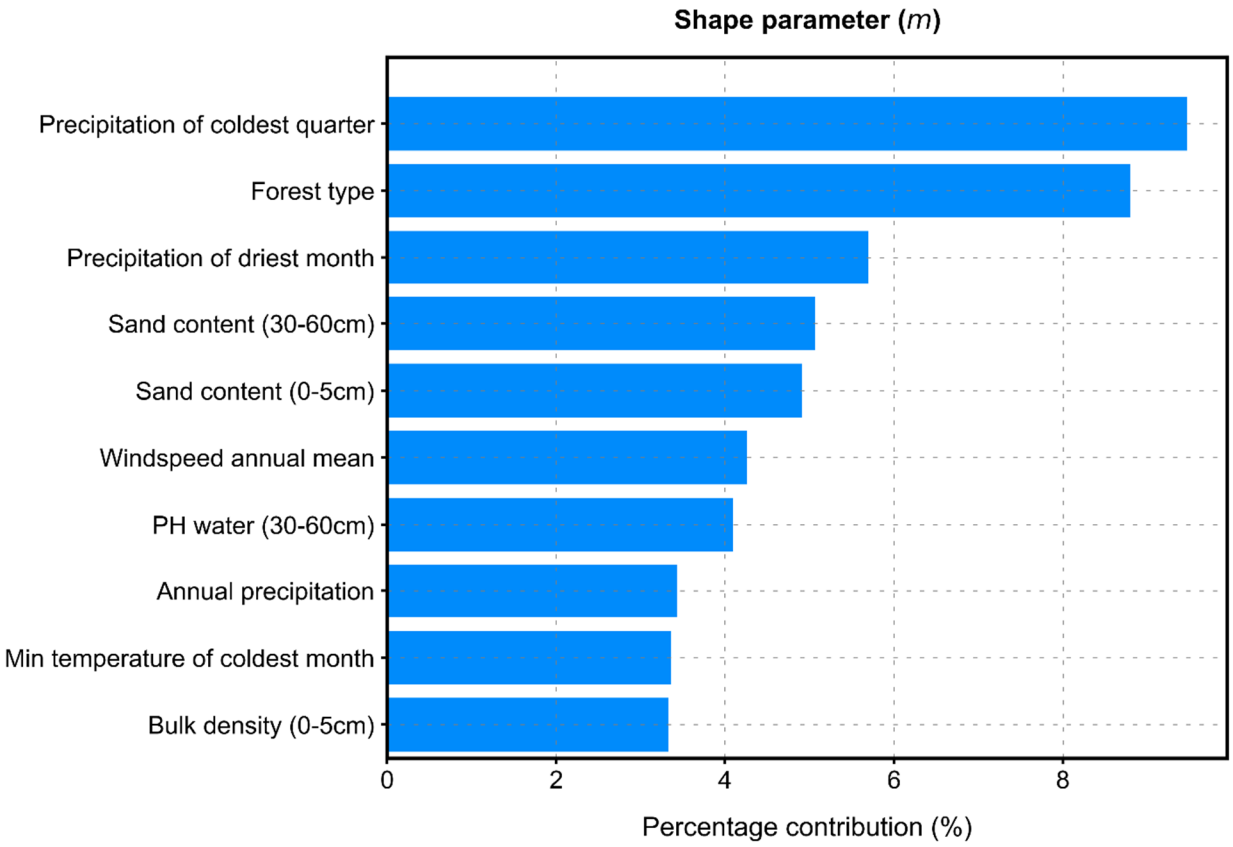

Fig S19: The percentage contributions of the top 10 covariates to the spatial variation of the *m* parameter in the Chapman-Richards growth function. The *m* parameter represents shape of the growth function.

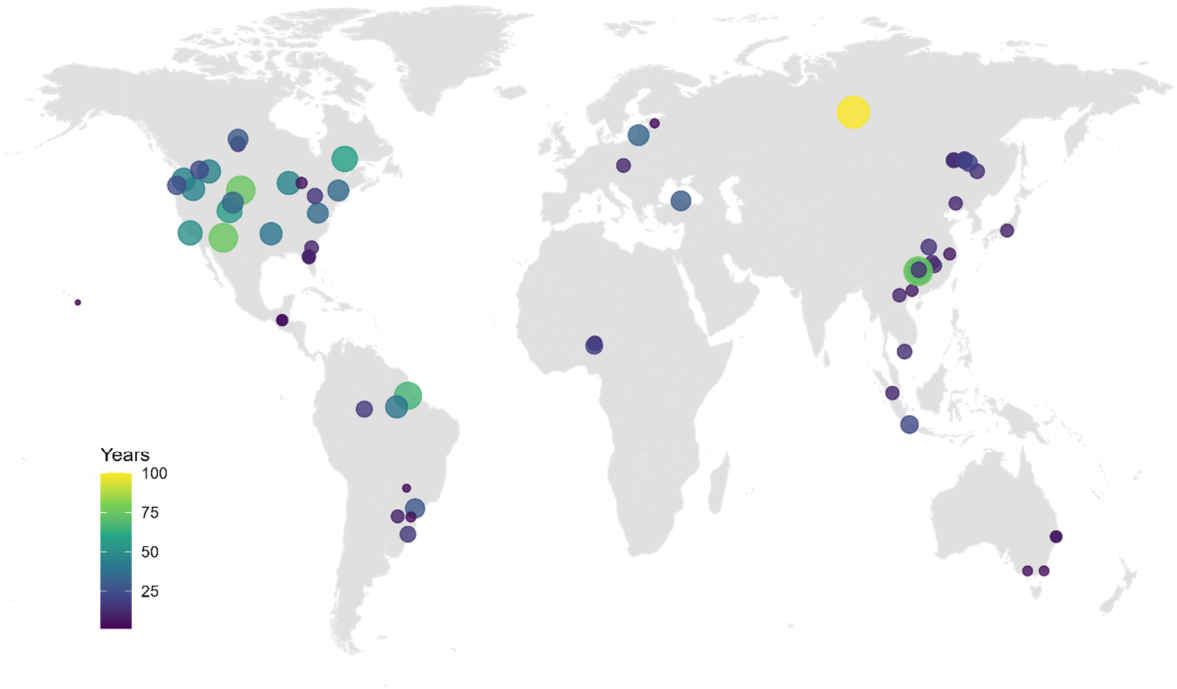

Fig S20: The spatial distribution of global synthesized data of forest peak growth age.

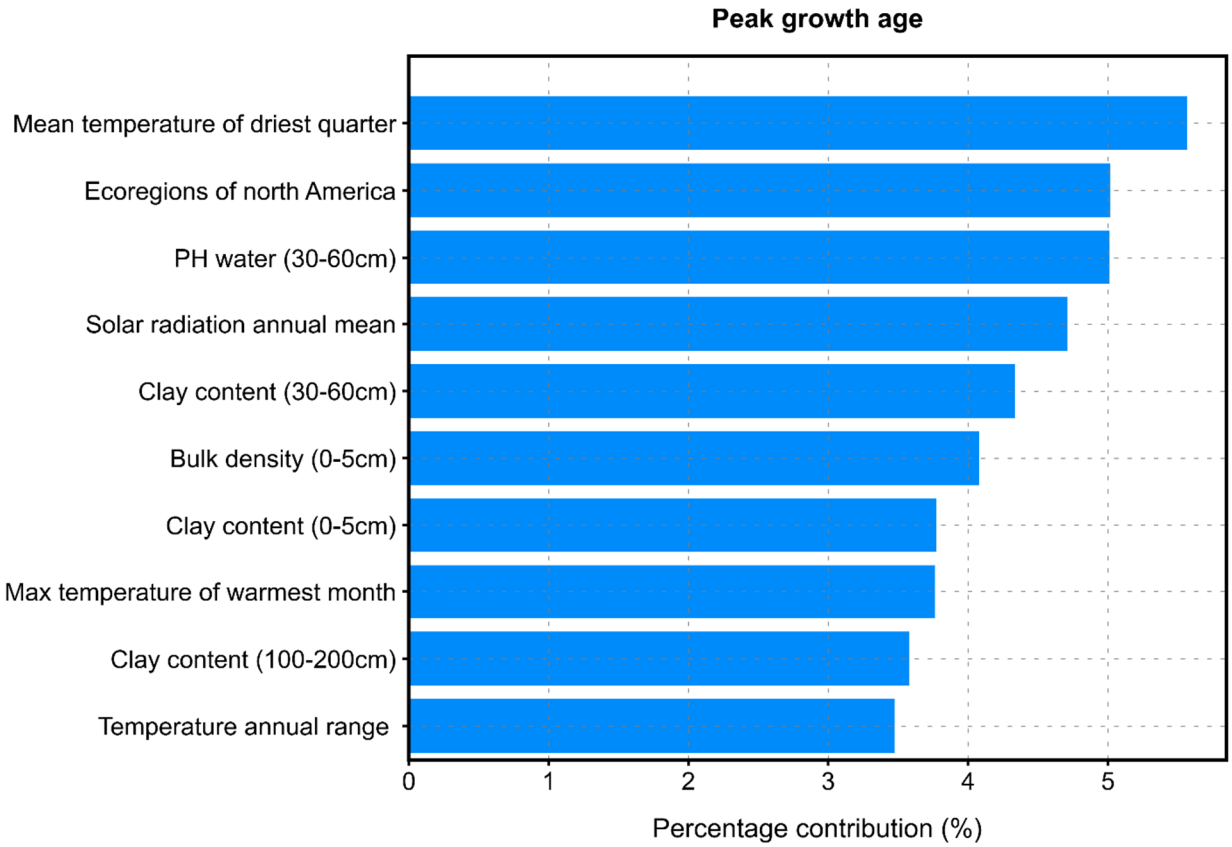

Fig S21: The percentage contributions of the top 10 covariates to the spatial variation of the predicted peak growth age.

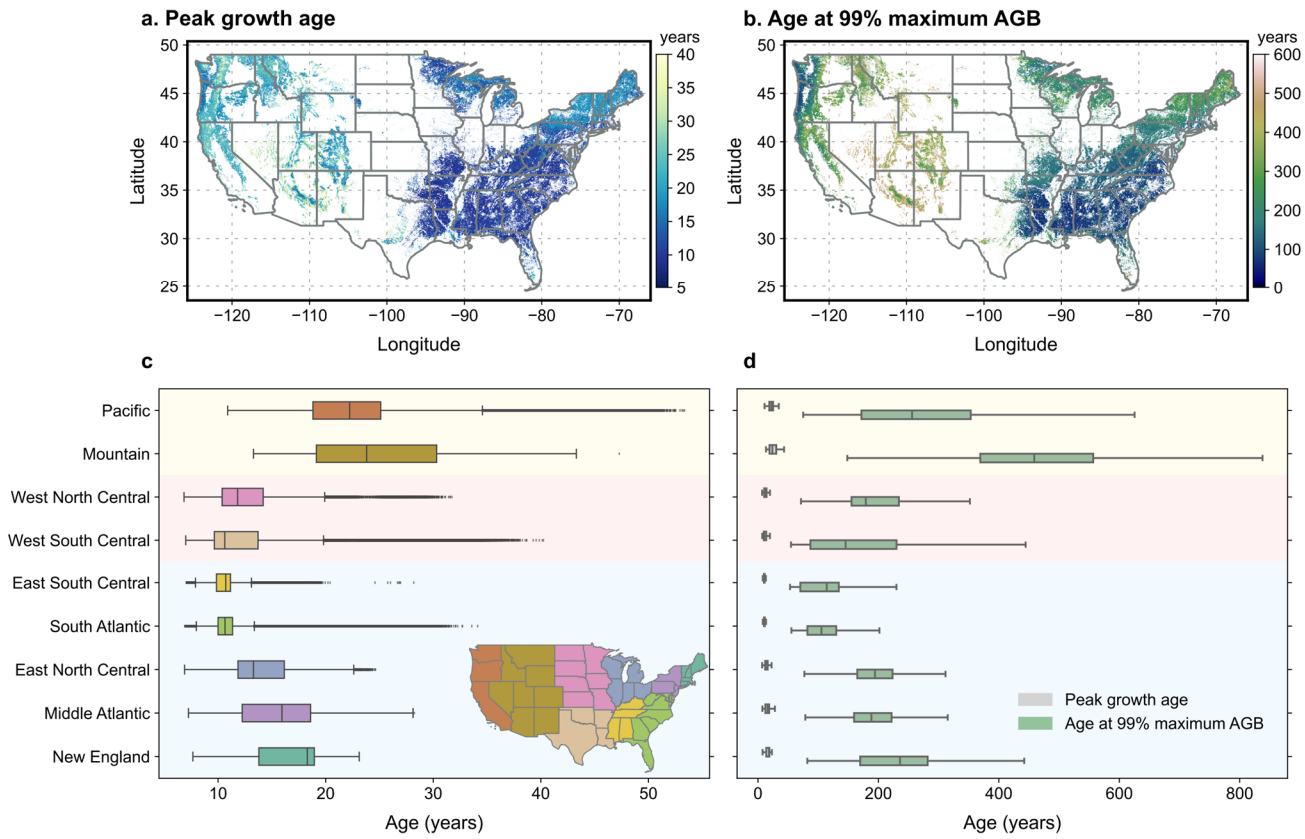

Fig. S22: Peak growth age and the age at which forests approach their maximum aboveground biomass (AGB) across the conterminous US. a, b. Spatial distributions of forest peak growth age (a) and the age at which forests reach 99% of their maximum AGB (b). **c.** Box plots of forest peak growth age for all pixels within nine US divisions[1]. The locations of each division are displayed on the inset map. **d.** Comparison of peak growth age (gray box plots) and age at 99% maximum AGB (green box plots) across the nine divisions.

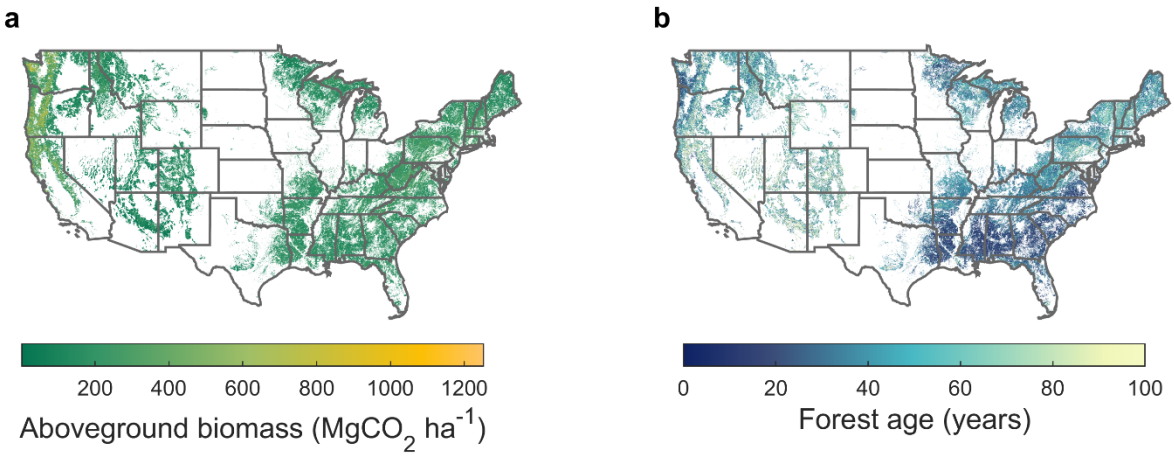

Fig S23: Spatial distributions of current aboveground biomass (a) and forest age (b).

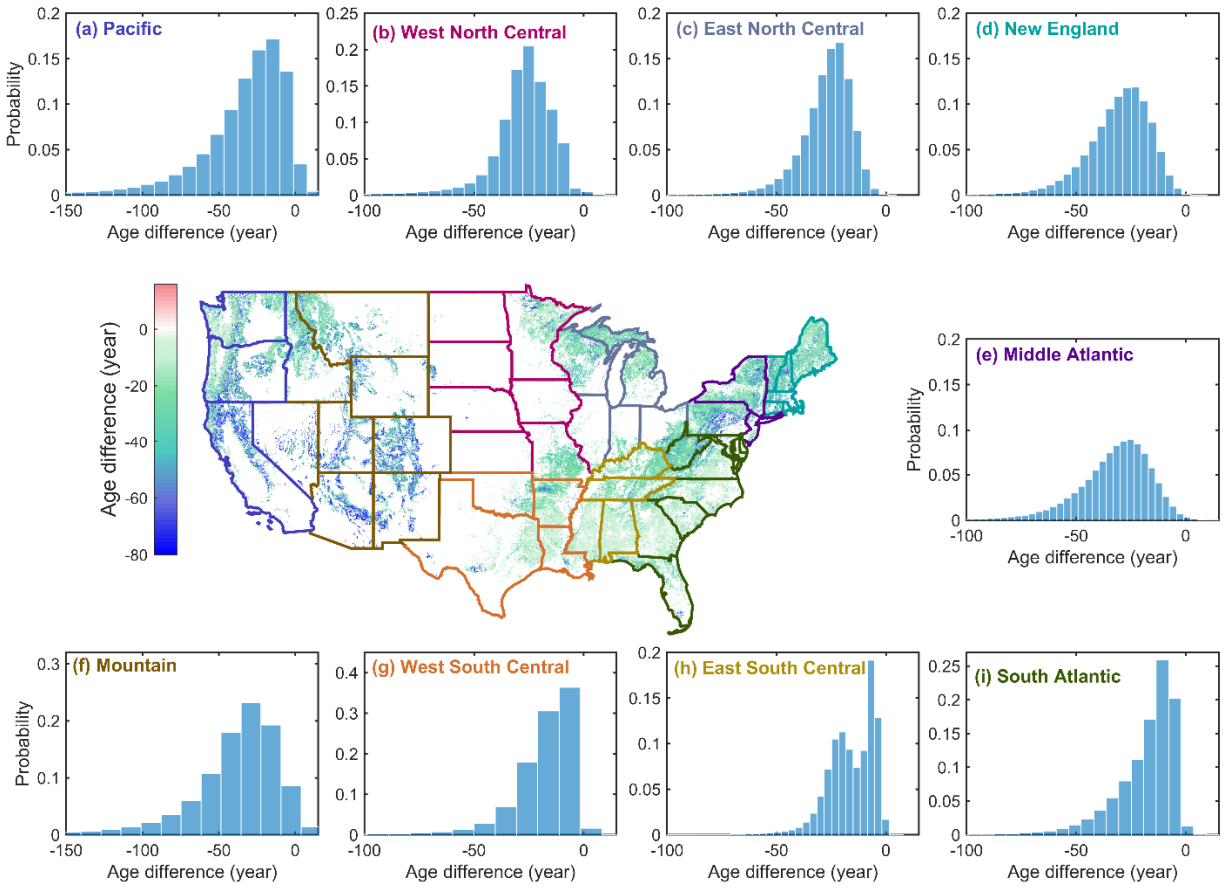

Fig S24: Regional variation in the age difference between peak growth age and current forest age across the conterminous US. The central map displays the spatial distribution of age differences, where negative values indicate that the current forest age exceeds the peak growth age, while positive values indicate that the current forest age is below the peak growth age. The map of current forest age is shown in Fig S23. The US is divided into 9 regions based on the Census Bureau's classification, with each region outlined in a distinct color. Panels (a–i) present histograms of the age difference distribution for each region, with label colors corresponding to the border colors on the central map.

Table S1: 46 covariates used in the Biogeochemistry-Informed Neural Network (BINN)

Variables	Types	Source
Lat	Geography	TreeMap 2016[2]
Lon	Geography	TreeMap 2016[2]
Ecoregions of North America	Categorical layer	https://www.epa.gov/eco-research/level-iii-and-iv-ecoregions-continental-united-states
Forest type	Categorical layer	TreeMap 2016[2]
BIO1 = Annual Mean Temperature	Bioclimatic	Ref[3]
BIO2 = Mean Diurnal Range (Mean of monthly (max temp - min temp))	Bioclimatic	
BIO3 = Isothermality (BIO2/BIO7) (×100)	Bioclimatic	
BIO4 = Temperature Seasonality (standard deviation ×100)	Bioclimatic	
BIO5 = Max Temperature of Warmest Month	Bioclimatic	
BIO6 = Min Temperature of Coldest Month	Bioclimatic	
BIO7 = Temperature Annual Range (BIO5-BIO6)	Bioclimatic	
BIO8 = Mean Temperature of Wettest Quarter	Bioclimatic	
BIO9 = Mean Temperature of Driest Quarter	Bioclimatic	
BIO10 = Mean Temperature of Warmest Quarter	Bioclimatic	
BIO11 = Mean Temperature of Coldest Quarter	Bioclimatic	
BIO12 = Annual Precipitation	Bioclimatic	
BIO13 = Precipitation of Wettest Month	Bioclimatic	
BIO14 = Precipitation of Driest Month	Bioclimatic	
BIO15 = Precipitation Seasonality (Coefficient of Variation)	Bioclimatic	
BIO16 = Precipitation of Wettest Quarter	Bioclimatic	
BIO17 = Precipitation of Driest Quarter	Bioclimatic	
BIO18 = Precipitation of Warmest Quarter	Bioclimatic	
BIO19 = Precipitation of Coldest Quarter	Bioclimatic	
Solar radiation annual mean	Climate	Ref[4]
Windspeed annual mean	Climate	
Inter-annual standard deviation of cloud cover	Climate	
Intra-annual SD of cloud cover	Climate	
Annual mean of cloud cover	Climate	
Aridity index values	Climate	Ref[5]
Elevation	Topographic	Ref[6]
Aspect eastness	Topographic	
Aspect northness	Topographic	
Profile curvature	Topographic	
Roughness	Topographic	
Slop	Topographic	
Aspect cosine	Topographic	
Aspect sine	Topographic	
Bulk Density (0, 30 and 100 cm)	Soil	Ref[7]

Cation Exchange Capacity (0, 30 and 100 cm)	Soil
Clay Content (0, 30 and 100 cm)	Soil
Coarse Fragments Volumetric (0, 30 and 100 cm)	Soil
pH Water (0, 30 and 100 cm)	Soil
Sand Content (0, 30 and 100 cm)	Soil
Silt Content (0, 30 and 100 cm)	Soil
Soil Water Capacity (0, 30 and 100 cm)	Soil
Total nitrogen (0, 30 and 100 cm)	Soil

Table S2: List of 92 forest types from 26 forest groups used in this study. Numbers in parentheses indicate the forest type codes used in the FIA database.

Forest Type Group	Forest Type
White / red / jack pine group (100)	Jack pine (101) Red pine (102) Eastern white pine / eastern hemlock (104)
Spruce / fir group (120)	Balsam fir (121) White spruce (122) Red spruce (123) Red spruce / balsam fir (124) Black spruce (125) Tamarack (126) Northern white-cedar (127)
Longleaf / slash pine group (140)	Longleaf pine (141) Slash pine (142)
Loblolly / shortleaf pine group (160)	Loblolly pine (161) Shortleaf pine (162) Virginia pine (163) Sand pine (164)
Other eastern softwoods group (170)	Eastern redcedar (171)
Pinyon / juniper group (180)	Rocky Mountain juniper (182) Juniper woodland (184) Pinyon / juniper woodland (185)
Douglas-fir group (200)	Douglas-fir (201)
Ponderosa pine group (220)	Ponderosa pine (221) Jeffrey pine (225)
Fir / spruce / mountain hemlock group (260)	White fir (261) Noble fir (263) Pacific silver fir (264) Engelmann spruce (265) Engelmann spruce / subalpine fir (266) Grand fir (267) Subalpine fir (268) Mountain hemlock (270)
Lodgepole pine group (280)	Lodgepole pine (281)
Hemlock / Sitka spruce group (300)	Western hemlock (301) Western redcedar (304)
Western larch group (320)	Western larch (321)
Redwood group (340)	Redwood (341)

Other western softwoods group (360)	Western juniper (369)
California mixed conifer group (370)	California mixed conifer (371)
Exotic softwoods group (380)	Scotch pine (381)
Oak / pine group (400)	Eastern white pine / northern red oak / white ash (401) Eastern redcedar / hardwood (402) Longleaf pine / oak (403) Shortleaf pine / oak (404) Virginia pine / southern red oak (405) Loblolly pine / hardwood (406) Slash pine / hardwood (407) Other pine / hardwood (409)
Oak / hickory group (500)	Post oak / blackjack oak (501) Chestnut oak (502) White oak / red oak / hickory (503) White oak (504) Northern red oak (505) Yellow-poplar / white oak / northern red oak (506) Sweetgum / yellow-poplar (508) Bur oak (509) Yellow-poplar (511) Black walnut (512) Black locust (513) Southern scrub oak (514) Chestnut oak / black oak / scarlet oak (515) Cherry / white ash / yellow-poplar (516) Elm / ash / black locust (517) Red maple / oak (519) Mixed upland hardwoods (520)
Oak / gum / cypress group (600)	Swamp chestnut oak / cherrybark oak (601) Sweetgum / Nuttall oak / willow oak (602) Overcup oak / water hickory (605) Baldcypress / water tupelo (607) Sweetbay / swamp tupelo / red maple (608) Baldcypress / pondcypress (609)
Elm / ash / cottonwood group (700)	Black ash / American elm / red maple (701) River birch / sycamore (702) Cottonwood (703) Sycamore / pecan / American elm (705) Sugarberry / hackberry / elm / green ash (706) Red maple / lowland (708) Cottonwood / willow (709)
Maple / beech / birch group (800)	Sugar maple / beech / yellow birch (801) Black cherry (802) Hard maple / basswood (805) Red maple / upland (809)

Aspen / birch group (900)	Aspen (901) Paper birch (902) Gray birch (903) Balsam poplar (904) Pin cherry (905)
Alder / maple group (910)	Red alder (911) Bigleaf maple (912)
Western oak group (920)	California black oak (922) Canyon live oak (933)
Tanoak / laurel group (940)	Tanoak (941)
Other hardwoods group (960)	Pacific madrone (961)

Table S3: The synthesized data of forest peak growth age

Num	Reference	Lat	Lon	Forest type information	Peak age (yr)
1	Liu et al., (2025) [8]	41.2	121.36	*Populus*	10
2	Dong et al., (2024) [9]	48.07	128.13	*Pinus sylvestris var. mongolica*	13
3	Silinskas et al., (2024) [10]	55.79	21.49	*Picea abies*	34
4	Olmedo et al., (2023) [11]	-29.79	-51.15	*Pinus* sp.	16
5	Bahtiar et al., (2023) [12]	-6.18	106.82	*Peronema canescens*	22
6	Qu et al., (2023) [13]	28.38	113.91	*Cunninghamia lanceolata*	11.7
		27.73	114.65	*Cunninghamia lanceolata*	12.4
		31.66	112.88	*Cunninghamia lanceolata*	15.44
7	Birdsey et al., (2023) [14]	39	-79.5	Mixed	35
		43.95	-73.0667	Mixed	35
		34.5	-94.25	Mixed	40
		44.28	-118.78	Mixed	45
		45.56	-88.67	Mixed	45
		46.27	-121.82	Mixed	45
		48.03	-113.8	Mixed	45
		34.66	-119.75	Mixed	50
		39.55	-107.32	Mixed	55
		33.63	-109.28	Mixed	75
		44.00	-103.79	Mixed	75
8	Numata et al., (2022) [15]	0.53	101.45	*Elaeis guineensis*	10
9	Ramirez et al., (2022) [16]	31.5	-81.5	*Pinus elliottii*	11
10	Dantas et al., (2022) [17]	-0.05	-51.12	*Pentaclethra macroloba*	66
11	Du et al., (2022) [18]	50.49	120.84	*Larix gmelinii Rupr.*	9.8
		50.41	120.96	*Larix gmelinii Rupr.*	12
		50.44	120.71	*Larix gmelinii Rupr.*	14.3
		50.42	123.95	*Larix gmelinii Rupr.*	14.4
		50.49	124.15	*Larix gmelinii Rupr.*	17.2
		50.45	124.06	*Larix gmelinii Rupr.*	18.2
12	Resende et al., (2021) [19]	-24.28	-48.9	*Araucaria angustifolia*	27.7
13	Martínez-Ramos et al., (2021) [20]	16.06	-90.75	*Trema*	3
		16.06	-90.75	*Cecropia*	5.8
		16.06	-90.75	*Trichospermum*	6
14	Li et al., (2021) [21]	30.16	119.48	*Phyllostachys pubescens*	7
15	Cherico et al., (2020) [22]	48.35	-116.79	*Pinus monticolaDouglas ex D. Don*	23
16	Binkley et al., (2020) [23]	-19.96	-51.59	*Eucalyptus*	2
		-26.11	-50.21	*Eucalyptus*	4
17	Hepner et al., (2020) [24]	58.32	26.55	*Populus tremula L. x P. tremuloides Michx.*	3
18	Hickey et al ., (2019) [25]	45.55	-84.67	*Pinus resinosa Sol. ex Aiton*	6
19	Phan et al., (2019) [26]	9.36	105.25	*Rhizophora apiculata*	13

20	Martiník et al., (2018) [27]	49.31	16.73	*Betula pendula Roth*	11
21	Zhou et al., (2017) [28]	22.39	107.61	*Eucalyptus*	7
22	Wei et al., (2016) [29]	26.49	109.54	*Schima superba*	55
23	Hopkinson et al., (2016) [30]	53.9	-104.65	*Pinus banksiana Lamb.*	14
24	Kahriman et al., (2016) [31]	41.73	34.84	*Fagus orientalis*	30
25	Lucas et al., (2014) [32]	-2.41	-54.7	flooded várzea forests	40
26	Chen et al., (2013) [33]	49.86	125.5	northwest temperate conifer	20
27	Tschieder et al., (2012) [34]	-25.97	-54.37	*Pinus taeda*	9
28	Ogawa et al., (2012) [35]	35.18	137.55	*Chamaecyparis obtusa*	9.3
29	Do et al., (2011) [36]	21.38	103.63	*W. paniculata*	10
30	Peichl ET AL., (2010) [37]	42.77	-80.45	*Pinus strobus L.*	15
31	Forrester et al., (2010) [38]	-37.61	144.03	*Eucalyptus globulus*	4
32	Rossi et al., (2009) [39]	50.71	-71.05	*Picea mariana*	57
33	Zha et al., (2009) [40]	54.94	-104.65	*Pinus banksiana Lamb.*	30
34	Zhao et al., (2009) [41]	26.83	109.75	*Cunninghamia lanceolata*	15
35	Tumer et al., (2008) [42]	-30.3	153	*E. grandis*	5
		-30.3	153	*E. pilularis*	7
36	Schöngart et al., (2007) [43]	-2.9	-64.88	*F. insipida*	17
37	Ryan et al., (2004) [44]	19.84	-155.12	*Eucalyptus saligna*	1
38	Forrester et al., (2004) [45]	-37.59	149.19	*A. mearnsii*	4
39	Martin et al., (2004) [46]	29.66	-82.33	*Pinus taeda*	10
40	Binkley et al., (2004) [47]	45.06	-123.95	Pseudotsuga menziesii (Mirb.) Franco	25
41	Wirth et al., (2002) [48]	60.71	89.13	*Pinus sylvestris L.*	100
42	Jokela et al., (2000) [49]	29.5	-82.3	*PinuselliottiiEngelm.var.elliottii*	8
		29.5	-82.3	*Pinus taeda*	10
43	Long et al., (1992) [50]	41.360	-106.317	*Pinus contorta*	35
44	Adegbehin et al., (1988) [51]	11.1	7.7	*Eucalyptus tereticornis*	13
		10.616	7.516	*Pinus caribaea*	19.3

References

1 U.S. Census Bureau. Census Bureau Regions and Divisions with State FIPS Codes. https://www2.census.gov/geo/pdfs/maps-data/maps/reference/us_regdiv.pdf

2 Riley, K. L., Grenfell, I. C., Shaw, J. D. & Finney, M. A. TreeMap 2016 Dataset Generates CONUS-Wide Maps of Forest Characteristics Including Live Basal Area, Aboveground Carbon, and Number of Trees per Acre. *Journal of Forestry* **120**, 607-632 (2022).

3 Fick, S. E. & Hijmans, R. J. WorldClim 2: new 1-km spatial resolution climate surfaces for global land areas. *International Journal of Climatology* **37**, 4302-4315 (2017).

4 Wilson, A. M. & Jetz, W. Remotely Sensed High-Resolution Global Cloud Dynamics for Predicting Ecosystem and Biodiversity Distributions. *PLOS Biology* **14**, e1002415 (2016).

5 Zomer, R. J., Xu, J. & Trabucco, A. Version 3 of the Global Aridity Index and Potential Evapotranspiration Database. *Scientific Data* **9**, 409 (2022).

6 Amatulli, G. *et al.* A suite of global, cross-scale topographic variables for environmental and biodiversity modeling. *Scientific Data* **5**, 180040 (2018).

7 Hengl, T. *et al.* SoilGrids250m: Global gridded soil information based on machine learning. *PLOS ONE* **12**, e0169748 (2017).

8 Liu, W. *et al.* Comparative Study on Growth Characteristics and Early Selection Efficiency of Hybrid Offspring of Populus deltoides 'DD-109' and P. maximowiczii in Liaoning, China. *Plants-Basel* **14**,111 (2025).

9 Dong, J. Y., Li, G. C., Liu, D. D., Wang, W. F. & Jiang, L. C. Use of a Carbon Density Growth Model to Assess the Potential Carbon Sink Function of a Mongolian Pine Plantation in Heilongjiang Province, Northeast China. *Forests* **15,** 2073 (2024).

10 Silinskas, B., Linkevicius, E., Aleinikovas, M., Beniusiene, L. & Skema, M. The Impact of Different Thinning Regimes on the Growth Dynamics of Pure Norway Spruce Stands in Lithuania. *Forests* **15,** 1791 (2024).

11 Olmedo, G. M. *et al.* Growth dynamic and climate signals on abandoned plantation of Pinus elliottii in Southern Brazil: A dendrochronological contribution. *Dendrochronologia* **82**, 126136 (2023)

12 Bahtiar, E. T. & Iswanto, A. H. Annual Tree-Ring Curve-Fitting for Graphing the Growth Curve and Determining the Increment and Cutting Cycle Period of Sungkai (Peronema canescens). *Forests* **14,** 1643 (2023).

13 Qu, Y. C. *et al.* Does the peak time of stand leaf area equal the biological maturity age of forests? *Forest Ecology and Management* **538**, 120988 (2023)

14 Birdsey, R. A. *et al.* Assessing carbon stocks and accumulation potential of mature forests and larger trees in US federal lands. *Frontiers in Forests and Global Change* **5**, 1074508 (2023).

15 Numata, I. *et al.* Deforestation, plantation-related land cover dynamics and oil palm age-structure change during 1990-2020 in Riau Province, Indonesia. *Environmental Research Letters* **17**, 094024 (2022).

16 Ramirez, L., Montes, C. R. & Bullock, B. P. Long-term term effect of bedding and vegetation control on dominant height of slash pine plantations in the southeastern United States. *Forest Ecology and Management* **522**,120479 (2022).

17 Dantas, A. R., Guedes, M. C., Lira-Guedes, A. C., Schöngart, J. & Piedade, M. T. F. Demographic and growth patterns of Pentaclethra macroloba (Willd.) Kuntze, a hyperdominant tree in the Amazon River estuary. *Population Ecology* **64**, 161-175 (2022).

18 Du, E. Z. & Tang, Y. Distinct Climate Effects on Dahurian Larch Growth at an Asian Temperate-Boreal Forest Ecotone and Nearby Boreal Sites. *Forests* **13**, 27 (2022)

19 Resende, R. T. *et al.* Age trends in genetic parameters for growth performance across country-wide provenances of the iconic conifer tree Araucaria angustifolia show strong prospects for systematic breeding and early selection. *Forest Ecology and Management* **501**, 119671 (2021)

20 Martínez-Ramos, M., Gallego-Mahecha, M. D., Valverde, T., Vega, E. & Bongers, F. Demographic differentiation among pioneer tree species during secondary succession of a Neotropical rainforest. *Journal of Ecology* **109**, 3572-3586 (2021).

21 Li, C. *et al.* Effects of different planting approaches and site conditions on aboveground carbon storage along a 10-year chronosequence after moso bamboo reforestation. *Forest Ecology and Management* **482**, 118867 (2021).

22 Cherico, J. R., Nelson, A. S., Jain, T. B. & Graham, R. T. Multidecadal Growth of Western White Pine and Interior Douglas-Fir Following Site Preparation. *Forests* **11**, 509 (2020).

23 Binkley, D., Campoe, O. C., Alvares, C. A., Carneiro, R. L. & Stape, J. L. Variation in whole-rotation yield among Eucalyptus genotypes in response to water and heat stresses: The TECHS project. *Forest Ecology and Management* **462**, 117953 (2020).

24 Hepner, H. *et al.* Effect of Early Thinning Treatments on Above-Ground Growth, Biomass Production, Leaf Area Index and Leaf Growth Efficiency in a Hybrid Aspen Coppice Stand. *Bioenergy Research* **13**, 197-209 (2020).

25 Hickey, L. J. *et al.* Contrasting Development of Canopy Structure and Primary Production in Planted and Naturally Regenerated Red Pine Forests. *Forests* **10**, 566 (2019).

26 Phan, S. M., Nguyen, H. T. T., Nguyen, T. K. & Lovelock, C. Modelling above ground biomass accumulation of mangrove plantations in Vietnam. *Forest Ecology and Management* **432**, 376-386 (2019).

27 Martiník, A., Knott, R., Krejza, J. & Cerny, J. Biomass production of Betula pendula stands regenerated in the region of allochthonous Picea abies dieback. *Silva Fennica* **52**, 9985 (2018)

28 Zhou, X. G. *et al.* Optimal rotation length for carbon sequestration in Eucalyptus plantations in subtropical China. *New Forests* **48**, 609-627 (2017).

29 Wei, H., Deng, X., Ouyang, S., Chen, L. & Chu, Y. Growth process and model simulation of three different classes of Schima superba in a natural subtropical forest in China. *IOP Conference Series: Earth and Environmental Science* **52**, 012106 (2017).

30 Hopkinson, C. *et al.* Monitoring boreal forest biomass and carbon storage change by integrating airborne laser scanning, biometry and eddy covariance data. *Remote Sensing of Environment* **181**, 82-95 (2016).

31 Kahriman, A., Altun, L. & Güvendi, E. Determination of stand structure in even-aged Oriental Beech Forests in Turkey. *Bosque* **37**, 557-569 (2016).

32 Lucas, C. M. *et al.* Effects of land-use and hydroperiod on aboveground biomass and productivity of secondary Amazonian floodplain forests. *Forest Ecology and Management* **319**, 116-127 (2014).

33 Chen, B. *et al.* Evaluating the impacts of climate variability and disturbance regimes on the historic carbon budget of a forest landscape. *Agricultural and Forest Meteorology* **180**, 265-280 (2013).

34 Tschieder, E. F., Fernández, M. E., Schlichter, T. M., Pinazo, M. A. & Crechi, E. H. Influence of growth dominance and individual tree growth efficiency on Pinus taeda stand growth. A contribution to the debate about why stands productivity declines. *Forest Ecology and Management* **277**, 116-123 (2012).

35 Ogawa, K. Mathematical analysis of age-related changes in leaf biomass in forest stands. *Canadian Journal of Forest Research* **42**, 356-363 (2012).

36 Do, T. V. *et al.* Population changes of early successional forest species after shifting cultivation in Northwestern Vietnam. *New Forests* **41**, 247-262 (2011).

37 Peichl, M., Arain, M. A. & Brodeur, J. J. Age effects on carbon fluxes in temperate pine forests. *Agricultural and Forest Meteorology* **150**, 1090-1101 (2010).

38 Forrester, D. I., Collopy, J. J. & Morris, J. D. Transpiration along an age series of Eucalyptus globulus plantations in southeastern Australia. *Forest Ecology and Management* **259**, 1754-1760 (2010).

39 Rossi, S., Tremblay, M. J., Morin, H. & Savard, G. Growth and productivity of black spruce in even- and uneven-aged stands at the limit of the closed boreal forest. *Forest Ecology and Management* **258**, 2153-2161 (2009).

40 Zha, T. *et al.* Carbon sequestration in boreal jack pine stands following harvesting. *Global Change Biology* **15**, 1475-1487 (2009).

41 Zhao, M. F., Xiang, W. H., Peng, C. H. & Tian, D. L. Simulating age-related changes in carbon storage and allocation in a Chinese fir plantation growing in southern China using the 3-PG model. *Forest Ecology and Management* **257**, 1520-1531 (2009).

42 Tumer, J. & Lambert, M. J. Nutrient cycling in age sequences of two Eucalyptus plantation species. *Forest Ecology and Management* **255**, 1701-1712 (2008).

43 Schöngart, J. *et al.* Management criteria for Ficus insipida Willd.: (Moraceae) in Amazonian white-water floodplain forests defined by tree-ring analysis. *Annals of Forest Science* **64**, 657-664 (2007).

44 Ryan, M. G., Binkley, D., Fownes, J. H., Giardina, C. P. & Senock, R. S. An experimental test of the causes of forest growth decline with stand age. *Ecological Monographs* **74**, 393-414 (2004).

45 Forrester, D. I., Bauhus, J. & Khanna, P. K. Growth dynamics in a mixed-species plantation of Eucalyptus globulus and Acacia mearnsii. *Forest Ecology and Management* **193**, 81-95 (2004).

46 Martin, T. A. & Jokela, E. J. Stand development and production dynamics of loblolly pine under a range of cultural treatments in north-central Florida USA. *Forest Ecology and Management* **192**, 39-58 (2004).

47 Binkley, D. A hypothesis about the interaction of tree dominance and stand production through stand development. *Forest Ecology and Management* **190**, 265-271 (2004).

48 Wirth, C. *et al.* Comparing the influence of site quality, stand age, fire and climate on aboveground tree production in Siberian Scots pine forests. *Tree Physiology* **22**, 537-552 (2002).

49 Jokela, E. J. & Martin, T. A. Effects of ontogeny and soil nutrient supply on production, allocation, and leaf area efficiency in loblolly and slash pine stands. *Canadian Journal of Forest Research-Revue Canadienne De Recherche Forestiere* **30**, 1511-1524 (2000).

50 Long, J. N. & Smith, F. W. VOLUME INCREMENT IN PINUS-CONTORTA VAR LATIFOLIA - THE INFLUENCE OF STAND DEVELOPMENT AND CROWN DYNAMICS. *Forest Ecology and Management* **53**, 53-64 (1992).

51 Adegbehin, J. O., Okojie, J. A. & Nokoe, S. GROWTH OF EUCALYPTUS-TERETICORNIS AND PINUS-CARIBAEA AT DIFFERENT SITES IN NORTHERN NIGERIA. *Forest Ecology and Management* **23**, 261-272 (1988).